An integrated approach to investigate age-related modifications of morphological, mechanical and structural properties of type I collagen

Laurence van Gulick, Charles Saby, Stéphane Jaisson, Anaïs Okwieka, Philippe Gillery, Emilie Dervin, Hamid Morjani, Abdelilah Beljebbar

1

An integrated approach to investigate age-related modifications of morphological,

mechanical and structural properties of type I collagen

Laurence VAN GULICK[a], Charles SABY[a], Stéphane JAISSON[b], Anaïs OKWIEKA[b], Philippe GILLERY[b], Emilie DERVIN[a], Hamid MORJANI[a#], Abdelilah BELJEBBAR[a#*]

[a] BioSpectroscopie Translationnelle, EA 7506, Université de Reims Champagne-Ardenne, UFR de Pharmacie, 51 rue Cognacq-Jay, 51096 Reims CEDEX, France.

[b] Extracellular Matrix and Cell Dynamics Unit CNRS UMR 7369, Université de Reims Champagne-Ardenne, UFR de Médecine, 51 rue Cognacq-Jay, 51096 Reims CEDEX, France

*: Correspondence should be sent to:

Dr. Abdelilah BELJEBBAR
BioSpectroscopie Translationnelle, EA 7506
UFR de Pharmacie,
Université de Reims Champagne-Ardenne
51, rue Cognacq-Jay,
51096 Reims CEDEX, France

Phone: (33) 3 2691-8376
Fax: (33) 3 2691-8282
E-mail: abdelilah.beljebbar@univ-reims.fr

[#]HM and AB are co-senior authors on this work.

1

ABSTRACT

The main propose of this study is to characterize the impact of chronological aging on mechanical, structural, biochemical, and morphological properties of type I collagen. We have developed an original approach combining a stress-strain measurement device with a portable Raman spectrometer to enable simultaneous measurement of Raman spectra during stress vs strain responses of young adult, adult and old rat tail tendon fascicles (RTTF). Our data showed an increase in all mechanical properties such as Young modulus, yield strength, and ultimate tensile strength with aging. At the molecular level, Raman data revealed that the most relevant frequency shift was observed at 938 cm^{-1} in Old RTTFs, which is assigned to the C–C. This suggested a long axis deformation of the peptide chains in Old RTTFs during tensile stress. In addition, the intensity of the band at 872 cm^{-1}, corresponding to hydroxyproline decreased for young adult RTTFs and increased for the adult ones, while it remained unchanged for Old RTTF during tensile stress. The amide III band (1242 and 1265 cm^{-1}) as well as the band ratios I_{1631}/I_{1663} and I_{1645}/I_{1663} responses to tensile stress were depending on mechanical phases (toe, elastic and plastic). The quantification of Advanced glycation end products by LC/MS/MS and spectrofluorometry showed an increase in their content with aging. This suggested that the accumulation of such products was correlated to the alterations observed in the mechanical and molecular properties of RTTFs. Analysis of the morphological properties of RTTFs by SHG combined with CT-FIRE software revealed an increase in length and straightness of collagen fibers, whereas their width and wavy fraction decreased. Our integrated study model could be useful to provide additional translational information to monitor progression of diseases related to collagen remodeling in musculoskeletal disorders.

INTRODUCTION

Collagens are the most abundant proteins in mammals.[1] In addition to their mechanical functions in the musculoskeletal system and in other organs such as skin and lung, collagen play also a functional role as an extracellular matrix component which activates specific membrane receptors in tissues such as the two mentioned above. This activation will in turn induce several cellular signaling pathways and consequently affect cell phenotype [2,3]. The consequences of a wide range of mutations leading to abnormal structural organization of collagens have been extensively reported to induce several diseases [4].

According to World Health Organization (WHO), the global proportion of people over 60 is expected to increase from 12% to 22% by 2050, leading to changes in patterns of pathogenesis and diseases. In addition, several chronic diseases are diagnosed in patients aged 75 years and over. Several studies have reported the importance of aging in the genetic mechanisms of a majority of diseases. In fact, the accumulation of mutations during aging could result in an increase in cellular and organ dysfunctions [5]. Conversely, mutations can also cause disability that accelerates the aging process [6]. Aging can contribute also to non-mutational alterations in several tissues. In fact, non-enzymatic post-translational modifications occur especially in the extracellular matrix proteins which have a long half-life, like type I collagen and elastin. The consequences of such alterations in terms of physiopathology have been especially studied [7,8]. Several studies have reported the relationship between aging and infectious diseases. In fact, the risk of infection increases with age and has been associated to the immune system remodeling in elderly populations. [9]. Additionally, this has been associated to alterations which occur in the cross-talk between the immune luminal and microbiota in the intestinal epithelium. [10]. Indeed, the turnover of collagen varies from one tissue to another. the 15 years half-life value which was cited in the manuscript is reported in general and corresponds to the collagen in the skin. On the

other hand, the half-life of collagen in cartilage, for example, is much higher (around 117 years). In addition, this increase in the half-life of collagen has a direct impact on the level of accumulation of AGEs. [11]

Type I collagen is an important component of several organs (skin, lung, bone and connective tissues). It consists of three subunits, two α1 chains and one α2 chain. These 3 chains lead to a right triple helix containing more than 1000 amino acids measuring 300 nm long and 1.4 nm in diameter. Amino acid sequence of the subunits consists of a Gly-X-Y triplet repeats. X and Y correspond frequently to proline (Pro) and 4-hydroxyproline (Hyp) respectively [12]. During chronological aging, type I collagen undergoes nonenzymatic post-translational modifications such as glycation, that results in the formation of Advanced Glycation End-products (AGEs) [13]. These AGEs lead to an increase in collagen cross-links [14] , which have an impact on morphological properties of the protein [15] by increasing collagen fiber straightness and rigidity, and decreasing fiber length and width. We have recently identified the age-related changes in molecular organization of type I collagen by using polarized Second Harmonic Generation (SHG) and Raman microspectroscopy [16]. Our results demonstrated that Amide I, amide III bands and those related to proline and hydroxyproline are highly sensitive to polarization and age-related. The anisotropy degree revealed the increase of the collagen fibers alignment to the fascicle backbone axis from adult to old tendons. SHG data confirms the increase of fiber straightness with aging. All these modifications have a deep impact on the mechanical properties and degradability of type I collagen [17]. Raman spectroscopy combined to stress vs strain measurements is a powerful toll to investigate the molecular response of samples to external tensile stress. Previous studied have used Raman spectroscopy to monitor the molecular changes in collagenous tissues subjected to tensile strain [18–20]. Wang et al. have analyzed collagen fibers extracted from 5 months old Wistar rats. They explored the changes in frequency and

FWHM of two collagen bands at 879 and 822 cm^{-1} as a function of applied tensile strain. Gąsior-Głogowska et al. have investigated the changes in frequency of collagen bands of pig tail tendons upon mechanical test without specifying the age of the animals. In this previous study, mechanical tests and Raman spectra were performed on separate specimens and their corresponding results were correlated. Other studies showed that the increase in stiffness or Young's modulus was positively correlated to aging in the human Achilles [21] and mouse tibialis anterior [38] tendons. In addition to mechanical properties, aging has been found to affect also the turnover rate of collagen fibers in tail tendons fascicles [23,24]. The changes in tissue mechanical properties could be a combination between alteration of pre-existing collagen fibers and a progressive delay in their maturation, both dues to aging [25–27]. Viidik et al. have reported a clear relationship between mechanical properties of tendons (Young modulus) and age [28]. The age related changes in mechanical properties of other connective tissues have been correlated with their morphological and biochemical changes [29,30] and mechanical properties such as collagen density [16,31]

In the present work, we have investigated the relationship between the age-related changes in morphological, mechanical and structural properties of type I collagen from RTTFs using SHG, mechanical device and Raman spectroscopy respectively.

MATERIALS AND METHODS

Fifty RTTFs from young Adult (2 months, n=10), adult (4 months, n=10) and old (24 months, n=10) rats were analyzed (Figure 1). We have developed an original approach combining biomechanical device with portable Raman spectrometer to measure simultaneously mechanical properties of RTTFs (ultimate tensile strength, elasticity modulus and ultimate elongation, and strain rupture) and to identify the collagen bonds, in terms of Raman frequency and/or intensity, affected by a mechanical stress and aging. Biochemical analysis was performed on extracted collagen to quantify AGEs such as carboxymethyllysine (CML) and the nonenzymatic "cross-links" marker pentosidine. SHG was used to evaluate the morphological properties of collagen fibers such as width, length, waviness, and straightness.

Rat Tail Tendon fascicles

All animal procedures were approved by the ethical Committee for the use and care of animals of Reims Champagne-Ardenne (CEEA-RCA, registration number: 56, France) and the EU Directive 2010/63/EU. The animals were anesthetized with isoflurane and sacrificed. Tails were detached and then stored at -80 °C until further use. At day experiments, the skin was removed from the tails exposing all tendons, skeletal frame, and vascular system. To prevent tensile loading during tendon extraction, a flat clamp was used to hold the distal part of the tails. Fascicles were stored in the saline solution just for a few minutes to maintain they hydration and prevents the alteration in mechanical properties of tendon due to the long-term exposure to buffer solution.

Quantification of advanced glycation end-products (AGEs)

Type I collagen was extracted from rat tail tendons using 0.5 M acetic acid at 4°C, in the presence of protease inhibitors. Type I collagen was then specifically precipitated with NaCl 0.7

M. After centrifugation, the precipitate was re-suspended in 18 mM acetic acid, dialyzed against distilled water for 1 week at 4°C, to eliminate the salts used during the precipitation step, and lyophilized. [32]. CML and pentosidine quantification was performed on purified and lyophilized type I collagen using internal standard approach.[33] CML and pentosidine standards were purchased from IRIS biotech Gmbh (Marktredwitz, Germany). 1.4 mg of collagen (dry weight) was mixed with internal standards for CML or pentosidine and were submitted to acid hydrolysis (6 M HCl, final volume: 1 mL) at 110 °C for 18 h. Hydrolysates were evaporated to dryness twice under a nitrogen stream. The CML and pentosidine content of the collagen samples were then quantified by LC-MS/MS and expressed as nmol AGE/ g of collage.

For spectrofluorimetric analysis, collagen originated from Yg, Ad, and Old were solubilized at 3 mg/ml in 18 mM acetic acid (v/v), dialyzed against distilled water for 1 week at 4°C, to eliminate the salts used during the precipitation step, and lyophilized. Fluorescent AGEs were quantified using a spectrofluorimeter (Shimadzu model RF-500) at $\lambda ex = 380$ nm and $\lambda em = 440$ nm [34]. The fluorescence intensity was normalized to the dry weight of the sample. We have developed the standard addition method to quantify the fluorescent AGEs in type I collagen extracted from Yg, Ad, and Old using standard AGEs-BSA solution. Briefly, varying amounts of this standard solution were added to the solutions of collagen extracted from Yg, Ad, and Old. Fluorescence analysis was performed on each solution. Then the linear regression of calibration curve was used to calculate the concentration of the fluorescent AGES and expressed in mg AGEs/g of collagen.

SHG Analysis

SHG images were collected from different RTTFs with a Zeiss LSM 710-NLO microscope (Zeiss Microsystems, Marly le Roi, France) using a 20X objective (NA 0.8). Laser excitation at 860 nm was provided by a CHAMELEON femtosecond Titanium-Sapphire laser (Coherent, Courtaboeuf,

France). Laser power on the sample was adjusted up to 20 mW. RTTF samples were oriented by positioning the fiber long axis in the horizontal direction. Backward SHG images (425 μm × 425 μm) were collected from RTTFs with a 420–440 nm bandpass filter using ZEN imaging software. CT-FIRE, an open-source software package, was used to visualize and quantify the collagen fiber metrics. [35] Among these parameters, straightness was represented on a scale 0–1, where 1 corresponds to perfectly straight fibers. Length and width of collagen fibers were expressed in μm. Wavy fraction was calculated as the ratio of the number of fiber with waviness greater than 1.08 divided per the number of analyzed fibers. This parameter was expressed in a range from 0 to 1. The waviness is defined as the length of the collagen fiber (L_n) divided by the straight distance between the end-points (L_0) of this fiber (figure 2b).[36]

Mechanical tests

Tensile tests were carried out on a Deben MICROTEST 2KN testing machine (Deben UK Ltd., Edmunds, Suffolk, UK) equipped with a 20 N load cell (figure 2a). Fascicles were positioned on CaF2 windows, and immersion gel (Gel-larmes, Théa Pharma, Clermont-Ferrand) to maintain hydration during experiments [37]. The fascicle diameters were determined from microscope images. Fascicles were secured between grips (grip to grip distance: 20 mm) and were preloaded to a force level corresponding to 0.05N to remove slack [38]. The distance between the two grips lines was then measured to give the effective gauge length of the fascicle and defined as the start point. The fascicle strain during mechanical test was corrected accordingly. The stress-strain responses were measured on 50 Yg, Ad, and Old RTTFs at a constant speed of 0.1 mm/min.

Typical shape of stress-strain curve obtained by tensile tests is shown in figure 2b. Stress (in MPa) is calculated as the ratio of force applied on the fascicle (F in Newton) divided by its cross sectional area (S in m^2) (Stress =F/A). A set of mechanical properties can be extracted from such

curves. Young's modulus (MPa) was calculated as the slope of the linear portion of the stress-strain curve using a linear regression analysis. The ultimate tensile strength (UTS in MPa) is the maximum stress that the RTTF can withstand before failure. It defines the end of the plastic deformation phase. After this point the stress decreases until the complete rupture of the RTTF (elongation of rupture (in %). The Yield strength corresponding to the limit load at which the material begins to deform plastically. In the case of the tendon, the yield strength was determined by drawing the tangent to the stress vs strain curve and extending it to the x-axis. The initial point of the offset was thus determined. Then, by shifting this point by 0.2%, a line parallel to the tangent "Young's modulus" passing through this point was drawn. The Yield strength (in MPa) was obtained as the point of intersection between the stress vs strain curve and the offset parallel. Plastic phase range was determined between Yield point and UTS. The elastic region begins from the toe region ends to Yield point.

Raman spectroscopy

Raman spectra were recorded with a HE-785 commercial Raman spectrometer (Jobin-Vyon-Horiba, France) (figure 2a). This setup consisted of a high efficiency (HE) spectrometer with a fixed 950 g mm^{-1} grating coupled to a matrix charge coupled device (CCD) detector cooled by the Peltier effect at 200 K (Andor Technologies, South Windsor, CT, USA). A commercially available fiber probe (InPhotonics, Inc., Downy St, USA) was used to couple the excitation source and the detection system. This fiber probe is composed of a 100 μm diameter excitation fiber and a 100 μm diameter collection fiber. A bandpass filter, a beam splitter, a lens, a mirror, and a longpass filter were integrated in the compact probe head. This fiber probe, which has a focal distance of 5 mm, was mounted on a z-adjustable holder to optimize the focus on the sample and to ensure the good repeatability of acquisitions. The excitation source (785 nm) was

provided by an OEM diode laser (Process Instruments Inc., Salt Lake City, USA). The output power at the distal end of the excitation fiber was 120 mW. During stress-strain analysis, Raman spectra were recorded on the top of the fascicle at each applied stress. Each spectrum was acquired with 10 seconds integration time and five accumulations in the range from 500 to 3200 cm^{-1}. Data acquisition was performed using the Labspec 5.0 software (HORIBA Jobin Yvon). During stress-strain test, conventional Raman spectra were acquired on stretched RTTFs at each stress interval of 0.5 N. Total of 20 to 40 Raman spectra were recorded on each fascicle. At each age group, all spectra were grouped according to the stress applied.

Data processing and treatment

The processing of Raman data was performed with Matlab (Version 2018a, MathWorks). Various data processing steps were performed on raw measured spectra. The data pretreatment consisted of instrument response correction, wavenumber calibration, fluorescence background subtraction, cosmic ray removal.

Raman spectrum depends on the molecular composition of the sample and the response of the device. It is therefore essential to correct this response of the instrument in order to be able to compare directly the age-related changes in bands intensity of collagen with aging. The wavelength-dependent signal detection efficiency of the setup was measured using a calibration standard (standard reference material number-2241; NIST, Gaithersburg, MD, USA). Indeed, luminescence spectra of this material are acquired under the same conditions as the samples. These luminescence spectra are used to determine the intensity response curve of the instrument as a function of the wavenumbers. This curve is then used to calibrate the relative intensity of Raman spectra obtained on RTTFs with this spectrometer at 785 nm. Wavenumber calibration was performed using two Raman calibration standards, 4-acetamidophenol and cyclohexane,

along with the emission lines of the neon lamp. The cosmic rays were then removed and baseline correction was performed on Raman spectra using a fifth order polynomial fit. The spectrum of ophthalmic gel was recorded and subtracted from those measured on RTTFs.

The data were smoothed using a seven-point Savitzky–Golay algorithm. The resulting spectra were then normalized using a Standard Normal Variate (SNV) procedure. The second derivative spectra were calculated and used to identify the frequencies of underling sub-bands. From this analysis, A minimum in the second derivative of a spectrum corresponds to local frequencies of collagen bands in the original spectrum. Full width at half-maximum of these sub-bands were manually selected as the starting conditions. Curve fitting procedure was then applied using a mixed Gaussian and Lorentzian to estimate quantitatively the area of each Raman band intensities of collagen during tensile stress with aging. Comparisons of the χ^2 values and the residuals of the fits were used as the criteria for assessing the quality of fit.

Statistical analysis

Statistical analysis, using analysis of variance ANOVA followed by pairwise Tukey test, was performed on the intensity of the main characteristic Raman bands of type I collagen to find those bonds that were sensitive to the mechanical stress and aging. Statistical significance is represented with asterisks (*$p < 0.05$, **$p < 0.01$, ***$p < 0.001$).

RESULTS

Effect of aging on the biochemical properties of type I collagen

After acidic extraction of collagen from RTTFs, LC/MS/MS was used to quantify two AGEs known to be linked to the process of aging, namely CML and pentosidine. A significant increase in CML content was observed from Yg and Ad collagens to Old one with concentrations

of 35.93 ± 4.24, 41.43 ± 3.72, and 84.40 ± 5.52 nmol/g of collagen respectively ($p < 0.05$), (figure 3a). Pentosidine was not detected in Yg and Ad collagens (figure 3b), whereas its concentration was 0.41 ± 0.08 nmol/g ($p < 0.001$) in Old collagen. Additionally, fluorescent AGEs data from spectrofluorometry measurements showed a significant increase in AGE-FL content from Yg and Ad ($p < 0.001$) and between Yg and Old collagen ($p < 0.001$) with concentrations of 7.6 ± 0.7, 7.88 ± 1.20 and 18.45 ± 1.03 mg/g of collagen respectively (figure 3c). This increase in fluorescence and non-fluorescent AGE with aging may be the cause of reduced amounts of insoluble extracted collagen.

Morphological analysis of collagen fibers by SHG

The age-dependent modifications in collagen fiber organization were investigated using SHG microscopy (Figure 4a). Data showed that Yg RTTFs exhibited collagen fibers organized as periodic waveform with a long axis known as crimp morphology, indicating a low straightness. In addition, Yg RTTFs showed several dark regions due to inter-fascicle spaces delimiting fiber bundles. This pattern significantly changed in Ad and Old RTTFs. In fact, the collagen fibers became linear and parallel to backbone axis, whereas the number of dark regions decreased. In our previous study, we have reported that the average diameter of fascicles increased from Yg to Old RTT [39]. We have measured the mean diameter of Ad fascicles and complete the figure presented in our previous study in order to determine a statistically significant changes in diameter of fascicles between Yg, Ad, and old RTT. The average diameters of fascicles were 176 ± 13.0 µm, 230 ± 18.0 and 231 ± 26.0 µm for Yg, Ad, and Old respectively (figure 4c). The average diameter of tendon fascicles increased from Yg to Ad ($p<0.01$). No significant difference was observed in diameters of fascicles between Ad and Old RTTFs. A particular feature was observed in the SHG images of Old RTTFs (figure 4b), i.e. a feature named kink characterized by

fibril deformation or damage. This structure was present also in Ad RTTFs meaning that fiber kinks progressively accumulated with aging. Fast Fourier Transformed methods were also used to evaluate the local orientations of the fiber microstructure which characterizes orientation and anisotropy of RTTF microstructures. Vector maps showed the distribution of local fiber angulations. The analysis of these vector maps exhibited an alteration in some Ad and Old RTTF kink regions. Outside the kink regions, fibers remained parallel to the fascicle axis in Ad and old RTTFs. In Yg RTTFs, the vectors were normal to crimps. Taken together, vector maps data suggested that aging is characterized by the appearance of this kink structure due to fiber disorganization.

CT-FIRE software was used to quantify the statistical distribution and organization of collagen fibers in Yg, Ad, and Old RTTFs by extracting fiber metrics related to length, straightness, and width (figures 4d, 4e, 4f). The mean lengths of collagen fibers are displayed in figure 4d. The collagen fiber length expressed in µm was significantly lower in the Yg RTTFs (14.2 ± 2.0) when compared to Ad (16.9 ± 1.7) and Old RTTFs (17.6 ± 1.6) ($p<0.001$). No significant difference was observed in fiber lengths between Ad and Old RTTFs. Figure 4e showed a significant increase in collagen fiber straightness from Yg to Old collagen ($p<0.001$). Yg RTTFs exhibited a low straightness of collagen fibers (0.940 ± 0.005) with a waveform organization. In Ad and Old RTTFs, fibers become linear and oriented parallel to backbone axis (0.950 ± 0.005 and 0.960 ± 0.005 respectively). This indicates a high level of straightness in collagen fibers of Ad and Old RTTFs (figure 4e). Figure 4f displayed the evolution of the mean diameter of individual collagen fibers between Yg, Ad, and Old. The fiber diameter decreased significantly from 1.50 ± 0.08 (Yg) to 1.39 ± 0.06 (Ad), and 1.30 ± 0.05 µm (Old) ($p<0.001$) respectively. Finally, we have quantified the waviness property of collagen fibers in RTTFs. This was measured on 10 SHG

images of RTTFs (figure 4g). 10 fibers were selected per image and waviness was calculated by dividing the length of the fiber by the distance between the ends of each fiber. The wavy fraction was estimated as a percentage of fibers having waviness greater than 1.08. As shown in figure 4g, the wavy fraction of collagen fibers significantly decreased from Yg (0.34 ± 0.10) to Ad (0.04 ± 0.05), to Old (0) ($p < 0.001$).

Impact of aging on mechanical properties of collagen

Mechanical properties of RTTFs were investigated under uniaxial tensile loading direction parallel to the fiber axis. Figure 5a shows the mean values of stress vs strain measured on fifty RTTFs from each age. These stress *vs* strain curves were composed of three regions. The first region termed "toe" describes the behavior of RTTF at low deformation, where the collagen fiber crimps were straightened with a small increase in applied stress. The second region named "elastic phase" corresponds to a linear relationship between stress and strain, where the collagen fibers became fully oriented in the same direction as the load. In the last region named "plastic phase", the tendon reached its elastic limit where a little increase in stress causes a very important strain variation. The stress *vs* strain curves showed very a short plastic phase in Yg RTTFs and significantly increased in Ad and Old RTTFs (table 1). We then evaluated the changes in biomechanical parameters, Young Modulus, Yield stress, Ultimate tensile strength (UTS), and strain rupture of RTTFs with aging (figures 5b and 5c). The Young modulus was similar between Yg and Ad RTTFs (4.60 ± 0.55 MPa and 4.53 ± 0.73 MPa respectively) but significantly increased in Old ones (6.57 ± 1.50 MPa), with $p < 0.01$ and $p < 0.001$, respectively. This suggests an increase in the fascicle stiffness (figure 5b). The same behavior was observed for Yield strength, which significantly increased from Yg (6.75 ± 0.58 MPa) and Ad RTTFs (9.04 ± 0.93 MPa) to Old ones (31.30 ± 5.60 MPa) ($p < 0.001$) (figure 5c). The UTS of Yg RTTFs (7.95 ± 0.01

MPa) was comparable to that of Ad ones (10.82 ± 1.28 MPa), and significantly increased in Old RTTFs (36.65 ± 7.77 MPa, p<0.001) (figure 5c). Rupture strain significantly increased respectively in Ad (6.11 ± 0.59 %, p < 0.001) and Old (11.82 ± 1.59 %, p < 0.001) RTTFs, when compared to Yg (3.28 ± 0.26 %) (figure 5c). In addition, the rupture strain values were significantly different between Ad and Old RTTFs (p < 0.001).

We then investigated the impact of aging on elastic strain phase, plastic strain phase and plastic strength before the rupture (figure 5c). The elastic strain phase is similar between Yg (2.18 ± 0.32 %) and Ad RTTFs (2.55 ± 0.19 %). Moreover, this phase significantly increased from Ad to Old RTTFs (5.50 ± 0.32 %) (p<0.001) (figure 5d). Figure 5d displays the plastic strain phase, which significantly increased from Yg (1.80 ± 0.54 %) to Ad (2.50 ± 1.11 %) and Old RTTFs (5.50 ± 1.09 %) respectively (p<0.001). This phase significantly increased also from Ad to Old RTTFs (p<0.001). Significant difference was observed in plastic strength between Yg (0.60 ± 0.55 MPa) and Ad RTTFs (1.80 ± 0.73 MPa) (p<0.01) (figure 5d). This parameter significantly increased in Old RTTFs, when compared to both Yg and Ad ones (8.80 ± 1.51 MPa, p<0.001).

Characterization of structural–mechanical relationships of Type I collagen with aging by Raman spectroscopy

We have investigated the age-related structural alterations of collagen induced by mechanical stress. Raman spectra were acquired on RTTFs without and with gradually applied tensile stress. Figure 6a showed the mean Raman spectra of the unstrained Yg, Ad, and Old RTTFs. Table 2 listed the frequencies and tentative Raman bands assignments of the main characteristic bands of type I collagen. [40]. Briefly, the amide I vibration at 1663 cm^{-1} is dominated by peptide carbonyl stretching vibration with some contribution of C–N stretching and N–H in-plane bending. The amide III bands at 1265 and 1242 cm^{-1} arise from N–H bending and C–N stretching [41]. The

peak at 872 cm^{-1} is associated with the hydroxyproline ring. 851 and 920 cm^{-1} frequencies are assigned to the proline ring and the band at 938 cm^{-1} corresponds to the C–C stretching vibration of the collagen backbone.

Raman frequencies of the collagen bands did not undergo shifts with aging. However, we noticed changes in the intensities of the amide I and III bands and proline/hydroxyproline (851-938 cm^{-1}) between Yg, Ad, and Old. In fact, the relative intensity of the band at 851 cm^{-1} increased significantly from Yg to Ad RTTFs ($p<0.001$) (figure 6b). This band remains unchanged from Ad to Old RTTFs. The same behavior was observed for the band at 872 cm^{-1} ($p<0.01$). The vibration at 938 cm^{-1} is one of the most age-sensitive band of collagen. Its relative intensity increased significantly from Yg to Old RTTFs ($p<0.001$). The intensity of the band at 1265 cm^{-1} decreased with aging ($p<0.01$) (figure 6c), whereas the intensity of that at 1242 cm^{-1} increased from Yg to Ad ($p<0.01$) and to Old RTTFs ($p<0.001$) respectively. The intensity ratio 1265/1242 cm^{-1} was calculated to identify age-related variation in Amide III band (figure 6c). This ratio decreased significantly from Yg to Ad ($p<0.001$) and to Old RTTFs ($p<0.001$) respectively, and from Ad to Old RTTFs ($p<0.01$).

We have then investigated the age-related changes in the intensity and frequency of the Raman bands during mechanical stress. RTTFs were subjected to uniaxial tensile stress and Raman spectra were acquired during tensile stress. Figure 7a shows the frequency shift of Raman bands of hydroxyproline (872 cm^{-1}), proline (851 and 920 cm^{-1}), C–C stretching vibration of the backbone (938 cm^{-1}), and amide III bands (1265 and 1242 cm^{-1}) as a function of the mechanical stress. For Yg, Ad, and old RTTFs, the Raman bands at 851 and 872 cm^{-1} attributed to proline and hydroxyproline did not show any significant shift (less than 1 cm^{-1}) when stress force was applied. This suggests that these bands are not sensitive to the stretching (figure 7a). The most

relevant frequency shift was assigned to the C–C vibrations of the protein backbone at 938 cm^{-1} in Old RTTFs which suggests a long axis deformation of the peptide chains. In fact, gradual negative Raman shift was observed during stretching for Old RTTF from toe to plastic phases. However, this band did not show any pronounced changes in terms of frequency in Yg and Ad RTTFs during stretching. No significant shift in frequency of Amide III band (1242 and 1265 cm^{-1}) was observed for Yg and Ad RTTFs during tensile stress. However, the behavior of these two bands during stretching was completely different for Old RTTFs. In fact, positive frequency shift was observed for the band at 1242 cm^{-1} from toe to plastic phase, while the frequency at 1265 cm^{-1} shifted negatively. Furthermore, the frequency shift of this band was more pronounced than that of 1242 cm^{-1} in the plastic phase.

Figure 7b displays the variation in Raman band intensities of collagen during tensile stress with aging. The intensity of the band at 851 cm^{-1} was not sensitive to mechanical stress in Yg and Ad RTTFs. The band at 872 cm^{-1} decreased for Yg RTTFs, and increased for the Ad ones, while it remained unchanged for Old RTTF during tensile stress. The band at 938 cm^{-1} showed similar response to mechanical stress for Yg, Ad, and Old RTTFs. In fact, the intensity of this band was decreased for the three ages. The amide III band (1242 and 1265 cm^{-1}) was also affected during stretching. The intensity of the band at 1242 cm^{-1} increased for Yg RTTFs in elastic and plastic phases but remained almost unchanged for Ad ones. However, for Old RTTFs, the intensity of this band decreased until the stress value of 10 MPa and then increased in the remaining part of this phase as well as in the plastic phase. An increase in the intensity of the band at 1265 cm^{-1} was observed for Yg and Old RTTFs from toe to plastic phases while this band remains insensitive to stress for the Ad ones. Additionally, the intensity of this band increased in plastic phase for Old RTTFs while it remained unchanged for Yg and Ad ones.

To provide insight into the age-related conformational changes in the secondary structure of collagen induced by mechanical stress, the amide I band was decomposed using the curve-fitting analysis (figure 8). The second derivative spectra of the amide I bands revealed six sub-bands with frequencies centered at 1603, 1631, 1645, 1663, 1684, and 1695 cm^{-1} assigned to the different collagen secondary structures (Figure 8a).[42] The area of each component was normalized with respect to the whole amide I band. This decomposition of the amide I band showed the changes in sub-band intensities in unloaded condition (figure 8b) and during mechanical stress (figure 8c) for different RTTFs. We focused the analysis on the sub-bands 1631 cm^{-1}, 1645 cm^{-1}, and 1663 cm^{-1} structures. For non-stretched RTTFs, the intensity contribution of the structure at 1631 cm^{-1} increased respectively from Yg to Ad ($p<0.01$) and to Old RTTFs ($p<0.001$) respectively, and from Ad to Old RTTFs ($p<0.01$) (figure 8b). The intensity contribution of the structure at 1645 cm^{-1} decreased with aging. In fact, this contribution decreased respectively from Yg to Ad ($p<0.05$) and to Old RTTFs ($p<0.01$). However, no significant variation was observed between Ad and Old RTTFs intensity contribution of the structure at 1645 cm^{-1}. The contribution of the structure at 1663 cm^{-1} decreased respectively from Yg to Ad ($p<0.05$), from Yg to Old ($p<0.001$), and from Ad to Old RTTFS ($p<0.01$). This suggests that aging is accompanied by changes in molecular organization of collagen in unloaded RTTFs.

We then analyzed the age-related changes in the secondary structure of collagen during mechanical stress (Figure 8c). The contribution of the structure at 1631 cm^{-1} initially increased until the middle of the elastic phase, and then decreased until the end of the plastic phase for Yg and Ad RTTFs. However, the contribution of this structure was not significantly modified in the case of Old RTTFs. The contribution of the structure at 1663 cm^{-1} did not exhibit significant changes during mechanical stress in Yg RTTFs. For Ad RTTFs, the contribution of this band

increased in elastic phase and remained unchanged in the plastic one. On the other hand, this band significantly decreased in elastic phase, and then increased during the plastic ones in old RTTFs. The band contribution ratio I_{1631}/ I_{1663} was then calculated for the different RTTFs. This ratio increased for Yg RTTFs during both elastic and plastic phases, whereas a less pronounced behavior was observed in the case of Ad ones (figure 8c). For old RTTFs, this ratio decreased during most of the elastic phase and then increased until the end of the plastic one. The contribution of the structure at 1645 cm^{-1} initially decreased until the middle of the elastic phase, and then increased until the end of the plastic phase for Yg and Ad RTTFs. However, for Old RTTFs, the contribution of this structure remained unchanged in the elastic phase and decreased in the plastic one. The band contribution ratio I_{1645} / I_{1663} highly decreased for Yg RTTFs, whereas it remained unchanged in the case of Ad and Old ones (figure 8c).

DISCUSSION

In this study, we investigated the age-related changes in biochemical, morphological, mechanical, and structural properties of type I collagen of RTTFs. We implemented a new setup combining a Raman spectrometer coupled with fiber probe and a mechanical testing device. Such integrated system enabled simultaneous collection of strain–stress response and Raman spectra during tensile stress. SHG imaging data showed that Yg RTTFs exhibited a periodic waveform organization along the fascicle backbone axis [16]. This organization had a tendency to disappear in Ad and Old RTTFs, adopting a straight form parallel to RTTFs axis [17]. In addition, vector maps of preferential collagen fiber orientation allowed the identification of a particular feature named kink in Ad and Old RTTFs. Previous studies reported that fatigue loading causes a this feature in collagen fibers and consequently tendon degeneration [43,44]. The absence of this structure in Yg suggests that the kinks could be associated to the alteration in

the organization of collagen fibers with aging. CT-FIRE software allowed to quantify from SHG images the collagen fiber metrics such as length, straightness, width, and wavy faction in label free manner [45]. Our data show that these parameters underwent significant changes with aging. In fact, length and straightness of collagen fibers increased with aging, while their width and wavy fraction decreased. The SHG technique was previously applied to study the impact of type I collagen organization changes in pathologies [46,47].

Aging is associated with several musculoskeletal pathologies often characterized by loss of cartilage resilience and reduced ligament elasticity that induces a partial loss of tissue function.[48,49] Such alterations could be also associated to the kink feature described above. However, this could be the case of musculoskeletal tissues subjected to the most mechanical stress to support the weight of the animal during its movements with aging. It is important to note that in our study, we used the model of the tail tendon of the animal, which is less confronted to the mechanical factors described previously with aging. Recently, another study also attributed such features to aging, and particularly to glycation process. In fact, the authors reported that the stiffness profile and kink feature of tendon from mice tail were more prevalent in young diabetic animals when compared to wild-type ones. Moreover, such profile was similar to that found in tendon from wild-type old mice.[50]

A buffer solution was used to maintain tissue hydration during mechanical testing. The buffer solution osmolarity influences the water content of the tissue, which subsequently has an effect on the mechanical properties [51–53]. A recent study has investigated the effect of buffer solution on the hydration rat tail tendon fascicles and their mechanical properties. They reported that PBS increases the tissue water content and decreases its tensile stiffness [54]. In addition, buffer components can diffuse into the tissue and affect its mechanical properties. Other studies carried out on tendons and ligaments have reported conflicting results: hydration of tendon fascicles in

PBS decreases their tensile modulus [55,56], whereas another study has reported that it increases the modulus is increased in this condition [57]. Han et al. have reported that mechanical behaviors and the response of such models to loading in isotonic and hypertonic PBS buffers results in completely different profiles [58]. All these observations show the importance of the buffer conditions under which the loading test is performed and the measurements are carried out, which could have consequences on the interpretation of the data. We therefore propose to use the ophthalmic gel as an alternative buffer solution that after long-term incubation can maintain tissue hydration without diffusion of the buffer components. This gel is used for hydration of the eye and its protection against allergies. In the experiments that we carry out, it avoids photo-thermal effects induced by the laser excitation during mechanical tests. Figure S1 showed raw Raman spectra measured on RTTF hydrated in ophthalmic gel and ophthalmic gel. Difference spectrum was calculated by subtracting Raman spectrum of RTTF from that measured on ophthalmic gel (in green). This result shows a low contribution of the ophthalmic gel in the Raman spectrum of RTTF as well as a low overlap between its Raman bands and those of collagen.

Collagen is a fibrous protein that exhibits age dependent modifications in its biochemical properties such as AGEs accumulation [59]. These changes have been further associated to the modification of the mechanical properties of collagen [60–62]. We therefore investigated changes in the mechanical properties of RTTFs associated with aging. Our data showed an increase in all fiber metrics related to the mechanical properties of collagen fascicles (UTS, strain rupture, Young Modulus, and Yield stress). Moreover, we have observed an increase in elastic and plastic phase intervals from Yg to Old. These data are in agreement with previous studies showing that aging may result in stiffer and more resilient tendons [26,63].

Concerning the relationship between the morphology and mechanical properties, the crimps geometry is responsible for the non-linear behavior of RTTF stress vs strain response. The effect of crimp patterns on mechanical behavior of collagen fibers has not been clearly described. During tensile stress, the initial response to the load is due to stretching of the collagen crimping within the toe region without any lengthening of the collagen fibers [64], and the secondary response is due to the elongation of the collagen network. Crimp disappearance was related to the alignment of collagen fibers in the direction of the loading axis [65,66]. Intrinsic factors such as age can cause changes in the collagen fiber crimp morphology. Biomechanical studies demonstrated that crimps of the tendon fascicles disappeared when they were slightly stretched [66–70]. This was associated with the alignment of crimped collagen fibers in the direction of the loading axis [65,66].

Previous studies have shown that the level of collagen AGEs affects the stress–strain curve (Young Modulus) [71,72]. This suggested that the presence of AGEs increases the stiffness of soft tissue. As for the morphological aspect, it is important to note that in our study, we carried out our investigations on the RTTFs, which are less subjected to stress (weight, movement) during the life of the animal, in comparison to other musculoskeletal systems. We thus can suggest, as reported by Stammers et al, that such changes in the mechanical stress response could be attributed to aging and more specifically to the biochemical remodeling during this chronological process (glycation and AGEs accumulation).[50] The authors used additionally a diabetic model, in which the response to stress has been investigated on tails tendon fascicles from mice and compared to that observed in wild-type animals. Their data clearly showed that the diabetic animals, which exhibited an increase in the level of collagen glycation, mechanical stress response close to that observed in the model of aging.[50] In a previous study, data

reported by Eriksen and co-workers showed that stiffening of mouse tail tendon was related to dietary AGEs.[73] In addition, another study suggested that alteration of collagen fiber mechanics could be attributed mainly to the cross-links generated by AGEs.[74,75] Our data showed that the Young modulus was similar between Young adult and Adult RTTFs but significantly increased in Old ones despite the progressive increase in AGEs such as CML from Young Adult to Old RTTFs. However, only pentosidine content exhibited an increase in old RTTFs whereas it remained non-detectable in Young Adult and Adult ones. This finding support the involvement of cross-linking AGEs in the alteration of the Young Modulus [50,74–76].

Our study also investigated the relationships between Raman band characteristics (frequency, relative intensity and the "full width at half-maximum") and aging during mechanical stress. In our study, we have investigated the age related the changes in six Raman bands of collagen (frequency and relative intensity) during tensile stress and the different mechanical phases. We did not take into account weak frequency shift because the spectral resolution of High Efficiency (HE) Raman spectrometer is of 6 cm^{-1}. We have monitored the behavior of these bands as a function of the different mechanical phases for each age group. Wang et al. have investigated the Raman shift of the bands at 879 and 822 cm^{-1} when strain was applied. used Raman spectrometer used in this study was equipped with a triple monochromator to record Raman spectra of soft tissueon RTT with high spectral resolution. They reported changes in the frequencies of two collagen bands at 879 and 822 cm^{-1} during tensile stress.

The collagen fiber structure is stabilized by means of indirect intra- and inter-chain hydrogen bonds involving water molecules and the carbonyl groups of amino acids and/or the hydroxyl groups of hydroxyproline residues [77,78]. Thus, the proportion of hydroxyproline residues plays an important role in collagen hydration. We monitored the age-related variations in the main

Raman bands of collagen (851, 872, 938, amide III and amide I) according to the tensile stress and aging. The intensities of the amide I and III bands and proline/hydroxyproline (851-938 cm^{-1}) changed from Yg to Old RTTF. Our data suggested also that the intensity of the band at 872 cm^{-1} increased from Yg to Ad and remained unchanged for Old RTTFs during mechanical stress.

RTTFS were subjected to unidirectional tensile stress parallel to the fascicle axis. During mechanical test, Raman spectra were recorded using a fiber probe (InPhotonics). This fiber is not equipped with polarizer and analyzer in the excitation and collection fibers paths respectively. All Raman spectra recorded with this fiber probe were considered to correspond to unpolarized measurements. Additional information on the orientation and organization of collagen requires the use of polarized Raman spectroscopy. A previous study reported a clear correlation between the intensity profile of the Raman spectrum of collagen and the orientation of collagen fibers, depending on the laser polarization [79]. In addition, our Inphotonic probe is equipped with a multimode fiber for laser excitation. The output of the laser is not polarized. In this case, the changes in the Raman intensity of some bands were interpreted in terms of molecular composition instead of structural organization. Masic et al. have investigated stress-induced changes in collagen orientation in tendon by Polarized Raman Spectroscopy [80]. They reported that the changes in the intensity of Raman bands are related to the orientation and polarization direction of the incident laser light.

Wang et al. have investigated the molecular changes in collagen fibers extracted from 5 months old Wistar rats and subjected to in vitro axial tension. Fibers were kept moistened with buffered saline solution. The elongation of the sample was achieved by rotating manually the micrometer head. At each nominal increment, 3 to 5 Raman spectra were measured using SPEX 1877 Raman spectrometer equipped with triple monochromator. Excitation source was provided by Argon-ion

laser at 514.5 nm with 6 mW laser power. In this study, two collagen bands 879 and 822 cm^{-1} were investigated in term of frequency shift and the changes in their corresponding FWHM as a function of applied tensile strain. In our study, we have studied the age-related changes in molecular structure of collagen using fifty Yg (2 months), Ad (4 months) and Old (24 months) RTTFs. Six Raman bands of collagen (851, 872, 938, amide III (1242 and 1265 cm^{-1}) and amide I (1663 cm^{-1}) were monitored as function of mechanical stress and at different mechanical phase. The amide I band was used to provide insight into the age-related conformational changes in the secondary structure of collagen induced by mechanical stress. During mechanical test using tensile testing stage, Raman spectra were acquired at a stress interval of 0.5 N at the same location on each RTTF using near infrared laser excitation at 785 nm. Total of 20 to 40 Raman spectra were recorded on each fascicle. Wang et al. reported that a maximum band frequency shift of the band at 879 cm^{-1} was obtained at the strain rupture. Our results demonstrated that this band frequency shift is less than 1 cm^{-1}. In fact, we did not take into account weak frequency shift because the spectral resolution of High Efficiency (HE) Raman spectrometer is of 6 cm^{-1}. However, an increase in the relative intensity of this band was observed during mechanical stress. In addition, we investigated whether there is a relationship between the age-related changes in biochemical properties (AGEs) of type I collagen and the alterations that could affect its morphological, mechanical and structural properties.. In addition, we investigated whether there is a relationship between the age-related changes in biochemical properties (AGEs) of type I collagen on one hand and the alterations that could affect its morphological, mechanical and structural properties on the other hand. Our study supported in the discussion section by works published earlier, especially those highlighting the direct link between AGEs (those generating cross-links in particular) and changes in mechanical properties of collagen, suggests that such biochemical changes could have an impact on the structural organization of collagen as revealed

by Raman spectroscopy. In our previous study, we have identified the age related changes in molecular organization of type I collagen using polarized Raman microspectroscopy on RTTFs without applying tensile stress [39]. These molecular changes could be also associated to the alterations observed in the mechanical properties of collagen during tensile stress.

At the structural level, mechanical properties depend greatly on the hydroxyproline residue [70]. In fact, hydroxyproline facilitates intermolecular binding through the hydrogen bonding in the triple helical structure in collagen. Therefore, hydroxyproline content improves mechanical stability of the collagen fibers [81]. Accordingly, low proportion of hydroxyproline residues in the gap region of collagen fibrils was associated to a higher flexibility [82]. Another study has demonstrated that a high modulus is associated with an increase in hydroxyproline content [83]. The effect of AGEs on the organization of collagen fibrils at the molecular level is not sufficiently documented [84]. Chow et al. have shown that the alignment of the triplet repeats Gly-Pro-Hyp confers a flexibility to the collagen fibril [85]. Bansode et al. hypothesized that AGEs could induce a disordering in the alignment of the triplets [86]. Thus, we suggest that such changes could affect the Raman signature of hydroxyproline.

CONCLUSION

In this study, we have investigated the age-related changes in biochemical, morphological, mechanical, and structural properties of type I collagen from hydrated RTTFs. The study demonstrated that the developed system combining Raman spectroscopy and a stretching device was useful to investigate the relationship between molecular organization and mechanical properties of collagen with aging. The use of flexible optical fiber probe for laser delivery and Raman collection allowed complete separation of the Raman setup and the stretching device.

Our data showed an alteration in all parameters related to the mechanical properties of collagen fascicles (UTS, strain rupture, Young Modulus, and Yield stress) with aging. Using SHG images and CT-FIRE software, we objectively visualized and quantified changes in the morphology and organization of collagen fibers with aging. In fact, length and straightness of collagen fibers increased with aging, while width and wavy fraction decreased. We then monitored the age-related variation of intensity and frequency in the main bands of Raman signature of collagen when RTTFs were subjected to tensile stress. Our data show for the first time a correlation between the changes in some of the Raman bands (intensity and/or frequency) and mechanical properties of collagen with aging. This innovative method could be useful to provide additional clinically relevant information to monitor progression of diseases related to the remodeling of extracellular matrix proteins in the connective tissues, and highlight a need to consider aging of these components for the management of elderly patients and their clinical follow-up.

AUTHOR CONTRIBUTIONS

H. M., A. B. Conception and design; L. V. G. and A. B. Development of methodology; L. V. G., C. S. and E. D. Acquisition of data; A. O., S. J., and P. G. Biochemical analysis; L. V. G., H. M., and A. B. Analysis and interpretation; L. V. G., C. S., H. M., and A. B. Writing of the manuscript

COMPETING INTERESTS

The authors declare no conflict of interest

DATA AVAILABILITY

The datasets generated during and/or analyzed during the current study are available from the corresponding author on reasonable request.

*REFERENCES***:**

[1]   W. Traub, K.A. Piez, The chemistry and structure of collagen, Adv Protein Chem. 25 (1971) 243–352.

[2]   S. Ricard-Blum, The Collagen Family, Cold Spring Harbor Perspectives in Biology. 3 (2011) a004978–a004978.

[3]   J. Bella, D.J.S. Hulmes, Fibrillar Collagens, in: D.A.D. Parry, J.M. Squire (Eds.), Fibrous Proteins: Structures and Mechanisms, Springer International Publishing, Cham, 2017: pp. 457–490.

[4]   C. Bonod-Bidaud, F. Ruggiero, Inherited Connective Tissue Disorders of Collagens: Lessons from Targeted Mutagenesis, in: D. Figurski (Ed.), Genetic Manipulation of DNA and Protein - Examples from Current Research, InTech, 2013.

[5]   S.R. Kennedy, L.A. Loeb, A.J. Herr, Somatic mutations in aging, cancer and neurodegeneration, Mechanisms of Ageing and Development. 133 (2012) 118–126.

[6]   R. Romero-Ortuno, R.A. Kenny, R. McManus, Collagens and elastin genetic variations and their potential role in aging-related diseases and longevity in humans, Experimental Gerontology. 129 (2020) 110781.

[7]   H.L. Birch, Extracellular Matrix and Ageing, Subcell. Biochem. 90 (2018) 169–190.

[8]   P. Gillery, S. Jaisson, Post-translational modification derived products (PTMDPs): toxins in chronic diseases?, Clinical Chemistry and Laboratory Medicine. 52 (2014).

[9]   K.A. Kline, D.M. Bowdish, Infection in an aging population, Current Opinion in Microbiology. 29 (2016) 63–67.

[10] T. Walrath, K.U. Dyamenahalli, H.J. Hulsebus, R.L. McCullough, J. Idrovo, D.M. Boe, R.H. McMahan, E.J. Kovacs, Age-related changes in intestinal immunity and the microbiome, J Leukoc Biol. 109 (2021) 1045–1061.

[11] N. Verzijl, J. DeGroot, S.R. Thorpe, R.A. Bank, J.N. Shaw, T.J. Lyons, J.W.J. Bijlsma, F.P.J.G. Lafeber, J.W. Baynes, J.M. TeKoppele, Effect of Collagen Turnover on the Accumulation of Advanced Glycation End Products, Journal of Biological Chemistry. 275 (2000) 39027–39031.

[12] J.K. Mouw, G. Ou, V.M. Weaver, Extracellular matrix assembly: a multiscale deconstruction, Nature Reviews Molecular Cell Biology. 15 (2014) 771–785.

[13] A. Simm, B. Müller, N. Nass, B. Hofmann, H. Bushnaq, R.-E. Silber, B. Bartling, Protein glycation — Between tissue aging and protection, Experimental Gerontology. 68 (2015) 71–75.

[14] V.M. Monnier, G.T. Mustata, K.L. Biemel, O. Reihl, M.O. Lederer, D. Zhenyu, D.R. Sell, Cross-Linking of the Extracellular Matrix by the Maillard Reaction in Aging and Diabetes: An Update on "a Puzzle Nearing Resolution," Annals of the New York Academy of Sciences. 1043 (2005) 533–544.

[15] D. Aït-Belkacem, M. Guilbert, M. Roche, J. Duboisset, P. Ferrand, G. Sockalingum, P. Jeannesson, S. Brasselet, Microscopic structural study of collagen aging in isolated fibrils using polarized second harmonic generation, Journal of Biomedical Optics. 17 (2012) 0805061–0805063.

[16] L. Van Gulick, C. Saby, H. Morjani, A. Beljebbar, Age-related changes in molecular organization of type I collagen in tendon as probed by polarized SHG and Raman microspectroscopy, Sci Rep. 9 (2019) 7280.

[17] P. Panwar, G. Lamour, N.C.W. Mackenzie, H. Yang, F. Ko, H. Li, D. Brömme, Changes in Structural-Mechanical Properties and Degradability of Collagen during Aging-associated Modifications, Journal of Biological Chemistry. 290 (2015) 23291–23306.

[18] M. Gąsior-Głogowska, M. Komorowska, J. Hanuza, M. Ptak, M. Kobielarz, Structural alteration of collagen fibres--spectroscopic and mechanical studies, Acta Bioeng Biomech. 12 (2010) 55–62.

[19] Y.N. Wang, C. Galiotis, D.L. Bader, Determination of molecular changes in soft tissues under strain using laser Raman microscopy, J Biomech. 33 (2000) 483–486.

[20] H. Zhou, C.S. Simmons, M. Sarntinoranont, G. Subhash, Raman Spectroscopy Methods to Characterize the Mechanical Response of Soft Biomaterials, Biomacromolecules. (2020).

[21] A. Turan, M.A. Teber, Z.I. Yakut, H.A. Unlu, B. Hekimoglu, Sonoelastographıc assessment of the age-related changes of the Achilles tendon, Med Ultrason. 17 (2015) 58–61.

[22] L.K. Wood, E.M. Arruda, S.V. Brooks, Regional stiffening with aging in tibialis anterior tendons of mice occurs independent of changes in collagen fibril morphology, J Appl Physiol (1985). 111 (2011) 999–1006.

[23] A.V. Everitt, J.R. Wyndham, D.J. Barnard, The anti-aging action of hypophysectomy in hypothalamic obese rats: Effects on collagen aging, age-associated proteinuria development and renal histopathology, Mechanisms of Ageing and Development. 22 (1983) 233–251.

[24] A.V. Everitt, N.J. Seedsman, F. Jones, The effects of hypophysectomy and continuous food restriction, begun at ages 70 and 400 days, on collagen aging, proteinuria, incidence of pathology and longevity in the male rat, Mechanisms of Ageing and Development. 12 (1980) 161–172.

[25] P.L. Blanton, N.L. Biggs, Ultimate tensile strength of fetal and adult human tendons, Journal of Biomechanics. 3 (1970) 181–189.

[26] G.A. Johnson, D.M. Tramaglini, R.E. Levine, K. Ohno, N.-Y. Choi, S.L.-Y. Woo, Tensile and viscoelastic properties of human patellar tendon, Journal of Orthopaedic Research. 12 (1994) 796–803.

[27] Y. Nakagawa, K. Hayashi, N. Yamamoto, K. Nagashima, Age-related changes in biomechanical properties of the Achilles tendon in rabbits, Eur J Appl Physiol Occup Physiol. 73 (1996) 7–10.

[28] A. Viidik, H.M. Nielsen, M. Skalicky, Influence of physical exercise on aging rats: II. Life-long exercise delays aging of tail tendon collagen, Mechanisms of Ageing and Development. 88 (1996) 139–148.

[29] K.M. Reiser, S.M. Hennessy, J.A. Last, Analysis of age-associated changes in collagen crosslinking in the skin and lung in monkeys and rats, Biochimica et Biophysica Acta (BBA) - General Subjects. 926 (1987) 339–348.

[30] H.G. Vogel, Influence of maturation and age on mechanical and biochemical parameters of connective tissue of various organs in the rat, Connect Tissue Res. 6 (1978) 161–166.

[31] D. a. D. Parry, G.R.G. Barnes, A.S. Craig, D.C. Phillips, A comparison of the size distribution of collagen fibrils in connective tissues as a function of age and a possible relation between fibril size distribution and mechanical properties, Proceedings of the Royal Society of London. Series B. Biological Sciences. 203 (1978) 305–321.

[32] C. Saby, H. Rammal, K. Magnien, E. Buache, S. Brassart-Pasco, L. Van-Gulick, P. Jeannesson, E. Maquoi, H. Morjani, Age-related modifications of type I collagen impair DDR1-induced apoptosis in non-invasive breast carcinoma cells, Cell Adh Migr. 12 (2018) 335–347.

[33] S. Trellu, A. Courties, S. Jaisson, L. Gorisse, P. Gillery, S. Kerdine-Römer, C. Vaamonde-Garcia, X. Houard, F.-P. Ekhirch, A. Sautet, B. Friguet, C. Jacques, F. Berenbaum, J. Sellam, Impairment of glyoxalase-1, an advanced glycation end-product detoxifying enzyme, induced by inflammation in age-related osteoarthritis, Arthritis Res Ther. 21 (2019) 18.

[34] C. Saby, E. Buache, S. Brassart-Pasco, H. El Btaouri, M.-P. Courageot, L. Van Gulick, R. Garnotel, P. Jeannesson, H. Morjani, Type I collagen aging impairs discoidin domain receptor 2-mediated tumor cell growth suppression., Oncotarget. 7 (2016) 24908–27.

[35] J.S. Bredfeldt, Y. Liu, C.A. Pehlke, M.W. Conklin, J.M. Szulczewski, D.R. Inman, P.J. Keely, R.D. Nowak, T.R. Mackie, K.W. Eliceiri, Computational segmentation of collagen fibers from second-harmonic generation images of breast cancer, Journal of Biomedical Optics. 19 (2014) 016007–016007.

[36] R. Rezakhaniha, A. Agianniotis, J.T.C. Schrauwen, A. Griffa, D. Sage, C.V.C. Bouten, F.N. van de Vosse, M. Unser, N. Stergiopulos, Experimental investigation of collagen waviness and orientation in the arterial adventitia using confocal laser scanning microscopy, Biomech Model Mechanobiol. 11 (2012) 461–473.

[37] G. Ducourthial, J. Affagard, M. Schmeltz, X. Solinas, M. Lopez-Poncelas, C. Bonod-Bidaud, R. Rubio-Amador, F. Ruggiero, J. Allain, E. Beaurepaire, M. Schanne-Klein, Monitoring dynamic collagen reorganization during skin stretching with fast polarization-resolved second harmonic generation imaging, J. Biophotonics. 12 (2019) e201800336.

[38] D.P. Beason, A.F. Kuntz, J.E. Hsu, K.S. Miller, L.J. Soslowsky, Development and evaluation of multiple tendon injury models in the mouse, Journal of Biomechanics. 45 (2012) 1550–1553.

[39] L. Van Gulick, C. Saby, H. Morjani, A. Beljebbar, Age-related changes in molecular organization of type I collagen in tendon as probed by polarized SHG and Raman microspectroscopy, Sci Rep. 9 (2019) 7280.

[40] B.G. Frushour, J.L. Koenig, Raman scattering of collagen, gelatin, and elastin, Biopolymers. 14 (1975) 379–391.

[41] M. Kazanci, P. Roschger, E.P. Paschalis, K. Klaushofer, P. Fratzl, Bone osteonal tissues by Raman spectral mapping: Orientation–composition, Journal of Structural Biology. 156 (2006) 489–496.

[42] R.W. Williams, A.K. Dunker, Determination of the secondary structure of proteins from the amide I band of the laser Raman spectrum, Journal of Molecular Biology. 152 (1981) 783–813.

[43] J.H. Shepherd, K. Legerlotz, T. Demirci, C. Klemt, G.P. Riley, H.R. Screen, Functionally distinct tendon fascicles exhibit different creep and stress relaxation behaviour, Proceedings of the Institution of Mechanical Engineers, Part H: Journal of Engineering in Medicine. 228 (2014) 49–59.

[44] S.E. Szczesny, C. Aeppli, A. David, R.L. Mauck, Fatigue Loading of Tendon Results in Collagen Kinking and Denaturation but Does Not Change Local Tissue Mechanics, J Biomech. 71 (2018) 251–256.

[45] Y. Liu, A. Keikhosravi, C.A. Pehlke, J.S. Bredfeldt, M. Dutson, H. Liu, G.S. Mehta, R. Claus, A.J. Patel, M.W. Conklin, D.R. Inman, P.P. Provenzano, E. Sifakis, J.M. Patel, K.W. Eliceiri, Fibrillar Collagen Quantification With Curvelet Transform Based Computational Methods, Frontiers in Bioengineering and Biotechnology. 8 (2020).

[46] C.R. Drifka, A.G. Loeffler, K. Mathewson, A. Keikhosravi, J.C. Eickhoff, Y. Liu, S.M. Weber, W.J. Kao, K.W. Eliceiri, Highly aligned stromal collagen is a negative prognostic factor following pancreatic ductal adenocarcinoma resection, Oncotarget. 7 (2016) 76197–76213.

[47] S.L. Best, Y. Liu, A. Keikhosravi, C.R. Drifka, K.M. Woo, G.S. Mehta, M. Altwegg, T.N. Thimm, M. Houlihan, J.S. Bredfeldt, E.J. Abel, W. Huang, K.W. Eliceiri, Collagen

organization of renal cell carcinoma differs between low and high grade tumors, BMC Cancer. 19 (2019) 490.

[48] A.J. Freemont, J.A. Hoyland, Morphology, mechanisms and pathology of musculoskeletal ageing, The Journal of Pathology. 211 (2007) 252–259.

[49] R. Gheno, J.M. Cepparo, C.E. Rosca, A. Cotten, Musculoskeletal Disorders in the Elderly, J Clin Imaging Sci. 2 (2012) 39.

[50] M. Stammers, I.M. Ivanova, I.S. Niewczas, A. Segonds-Pichon, M. Streeter, D.A. Spiegel, J. Clark, Age-related changes in the physical properties, cross-linking, and glycation of collagen from mouse tail tendon, J Biol Chem. 295 (2020) 10562–10571.

[51] C.A. Grant, D.J. Brockwell, S.E. Radford, N.H. Thomson, Tuning the Elastic Modulus of Hydrated Collagen Fibrils, Biophys J. 97 (2009) 2985–2992.

[52] A.H. Hoffman, D.R. Robichaud, J.J. Duquette, P. Grigg, Determining the effect of hydration upon the properties of ligaments using pseudo Gaussian stress stimuli, Journal of Biomechanics. 38 (2005) 1636–1642.

[53] G.M. Thornton, N.G. Shrive, C.B. Frank, Altering ligament water content affects ligament pre-stress and creep behavior, Journal of Orthopaedic Research. 19 (2001) 845–851.

[54] B.N. Safa, K.D. Meadows, S.E. Szczesny, D.M. Elliott, Exposure to buffer solution alters tendon hydration and mechanics, Journal of Biomechanics. 61 (2017) 18–25.

[55] H.R.C. Screen, V.H. Chhaya, S.E. Greenwald, D.L. Bader, D.A. Lee, J.C. Shelton, The influence of swelling and matrix degradation on the microstructural integrity of tendon, Acta Biomaterialia. 2 (2006) 505–513.

[56] H.R.C. Screen, J.C. Shelton, V.H. Chhaya, M.V. Kayser, D.L. Bader, D.A. Lee, The Influence of Noncollagenous Matrix Components on the Micromechanical Environment of Tendon Fascicles, Ann Biomed Eng. 33 (2005) 1090–1099.

[57] R.C. Haut, A.C. Powlison, The effects of test environment and cyclic stretching on the failure properties of human patellar tendons, Journal of Orthopaedic Research. 8 (1990) 532–540.

[58] W.M. Han, N.L. Nerurkar, L.J. Smith, N.T. Jacobs, R.L. Mauck, D.M. Elliott, Multi-scale Structural and Tensile Mechanical Response of Annulus Fibrosus to Osmotic Loading, Ann Biomed Eng. 40 (2012) 1610–1621.

[59] D.S. Jackson, J.P. Bentley, On the Significance of the Extractable Collagens, The Journal of Biophysical and Biochemical Cytology. 7 (1960) 37–42.

[60] T.T. Andreassen, H. Oxlund, C.C. Danielsen, The influence of non-enzymatic glycosylation and formation of fluorescent reaction products on the mechanical properties of rat tail tendons, Connect Tissue Res. 17 (1988) 1–9.

[61] C.C. Danielsen, T.T. Andreassen, Mechanical properties of rat tail tendon in relation to proximal-distal sampling position and age, Journal of Biomechanics. 21 (1988) 207–212.

[62] A. Galeski, J. Kastelic, E. Baer, R.R. Kohn, Mechanical and structural changes in rat tail tendon induced by alloxan diabetes and aging, J Biomech. 10 (1977) 775–782.

[63] R.E. Shadwick, Elastic energy storage in tendons: mechanical differences related to function and age, Journal of Applied Physiology. 68 (1990) 1033–1040.

[64] L.J. Gathercole, A. Keller, Crimp Morphology in the Fibre-Forming Collagens, Matrix. 11 (1991) 214–234.

[65] J. Diamant, A. Keller, E. Baer, M. Litt, R.G.C. Arridge, F.C. Frank, Collagen; ultrastructure and its relation to mechanical properties as a function of ageing, Proceedings of the Royal Society of London. Series B. Biological Sciences. 180 (1972) 293–315.

[66] K.A. Hansen, J.A. Weiss, J.K. Barton, Recruitment of Tendon Crimp With Applied Tensile Strain, Journal of Biomechanical Engineering. 124 (2002) 72–77.

[67] D.H. Elliott, STRUCTURE AND FUNCTION OF MAMMALIAN TENDON, Biological Reviews. 40 (1965) 392–421.

[68] A. Viidik, R. Ekholm, Light and electron microscopic studies of collagen fibers under strain, Z. Anat. Entwickl. Gesch. 127 (1968) 154–164.

[69] A. Viidik, Simultaneous mechanical and light microscopic studies of collagen fibers, Z. Anat. Entwickl. Gesch. 136 (1972) 204–212.

[70] F. Flandin, C. Buffevant, D. Herbage, A differential scanning calorimetry analysis of the age-related changes in the thermal stability of rat skin collagen, Biochimica et Biophysica Acta (BBA) - Protein Structure and Molecular Enzymology. 791 (1984) 205–211.

[71] R.C. Haut, Age-Dependent Influence of Strain Rate on the Tensile Failure of Rat-Tail Tendon, Journal of Biomechanical Engineering. 105 (1983) 296–299.

[72] G.K. Reddy, Cross-Linking in Collagen by Nonenzymatic Glycation Increases the Matrix Stiffness in Rabbit Achilles Tendon, Exp Diabesity Res. 5 (2004) 143–153.

[73] C. Eriksen, R.B. Svensson, J. Scheijen, A.M.F. Hag, C. Schalkwijk, S.F.E. Praet, P. Schjerling, M. Kjær, S.P. Magnusson, C. Couppé, Systemic stiffening of mouse tail tendon is related to dietary advanced glycation end products but not high-fat diet or cholesterol, Journal of Applied Physiology. 117 (2014) 840–847.

[74] G. Fessel, J. Wernli, Y. Li, C. Gerber, J.G. Snedeker, Exogenous collagen cross-linking recovers tendon functional integrity in an experimental model of partial tear, Journal of Orthopaedic Research. 30 (2012) 973–981.

[75] Y. Li, G. Fessel, M. Georgiadis, J.G. Snedeker, Advanced glycation end-products diminish tendon collagen fiber sliding, Matrix Biology. 32 (2013) 169–177.

[76] N. Verzijl, J. DeGroot, C.B. Zaken, O. Braun-Benjamin, A. Maroudas, R.A. Bank, J. Mizrahi, C.G. Schalkwijk, S.R. Thorpe, J.W. Baynes, J.W.J. Bijlsma, F.P.J.G. Lafeber, J.M.

TeKoppele, Crosslinking by advanced glycation end products increases the stiffness of the collagen network in human articular cartilage: A possible mechanism through which age is a risk factor for osteoarthritis, Arthritis & Rheumatism. 46 (2002) 114–123.

[77] Q. Zhang, K.L. Andrew Chan, G. Zhang, T. Gillece, L. Senak, D.J. Moore, R. Mendelsohn, C.R. Flach, Raman microspectroscopic and dynamic vapor sorption characterization of hydration in collagen and dermal tissue, Biopolymers. 95 (2011) 607–615.

[78] L. de Vasconcelos Nasser Caetano, T. de Oliveira Mendes, E. Bagatin, H. Amante Miot, J.L. Marques Soares, M.M. Simoes e Silva Enokihara, A. Abrahao Martin, In vivo confocal Raman spectroscopy for intrinsic aging and photoaging assessment, Journal of Dermatological Science. 88 (2017) 199–206.

[79] A. Bonifacio, V. Sergo, Effects of sample orientation in Raman microspectroscopy of collagen fibers and their impact on the interpretation of the amide III band, Vibrational Spectroscopy. 53 (2010) 314–317.

[80] A. Masic, L. Bertinetti, R. Schuetz, L. Galvis, N. Timofeeva, J.W.C. Dunlop, J. Seto, M.A. Hartmann, P. Fratzl, Observations of Multiscale, Stress-Induced Changes of Collagen Orientation in Tendon by Polarized Raman Spectroscopy, Biomacromolecules. 12 (2011) 3989–3996.

[81] A. Ghanaeian, R. Soheilifard, Mechanical elasticity of proline-rich and hydroxyproline-rich collagen-like triple-helices studied using steered molecular dynamics, Journal of the Mechanical Behavior of Biomedical Materials. 86 (2018) 105–112.

[82] R.D.B. Fraser, T.P. MacRae, A. Miller, E. Suzuki, Molecular conformation and packing in collagen fibrils, Journal of Molecular Biology. 167 (1983) 497–521.

[83] L.K. Wood, E. Kayupov, J.P. Gumucio, C.L. Mendias, D.R. Claflin, S.V. Brooks, Intrinsic stiffness of extracellular matrix increases with age in skeletal muscles of mice, J Appl Physiol (1985). 117 (2014) 363–369.

[84] J.C. Hadley, K.M. Meek, N.S. Malik, Glycation changes the charge distribution of type I collagen fibrils, Glycoconj J. 15 (1998) 835–840.

[85] W. Ying Chow, D. Bihan, C.J. Forman, D.A. Slatter, D.G. Reid, D.J. Wales, R.W. Farndale, M.J. Duer, Hydroxyproline Ring Pucker Causes Frustration of Helix Parameters in the Collagen Triple Helix, Sci Rep. 5 (2015) 12556.

[86] S. Bansode, U. Bashtanova, R. Li, J. Clark, K.H. Müller, A. Puszkarska, I. Goldberga, H.H. Chetwood, D.G. Reid, L.J. Colwell, J.N. Skepper, C.M. Shanahan, G. Schitter, P. Mesquida, M.J. Duer, Glycation changes molecular organization and charge distribution in type I collagen fibrils, Sci Rep. 10 (2020) 3397.

Figure 1

a

Raman Spectrometer

InPhotonics probe

Laser 785 nm

Excitation fiber

Collection fiber

Motor

Grip

Grip

Fascicle

CaF₂

Force transducer

Tensile Stage

b

Toe | Elastic phase | Plastic phase | Rupture

T | E | P | R

Stress (MPa)

UTS

Rupture strain

Yield strength

Young's modulus

Strain (%)

L_n

L_0

Raman intensity (A.U.)

Raman Acquisition

Wavenumber (cm^{-1})

600 800 1000 1200 1400 1600 1800
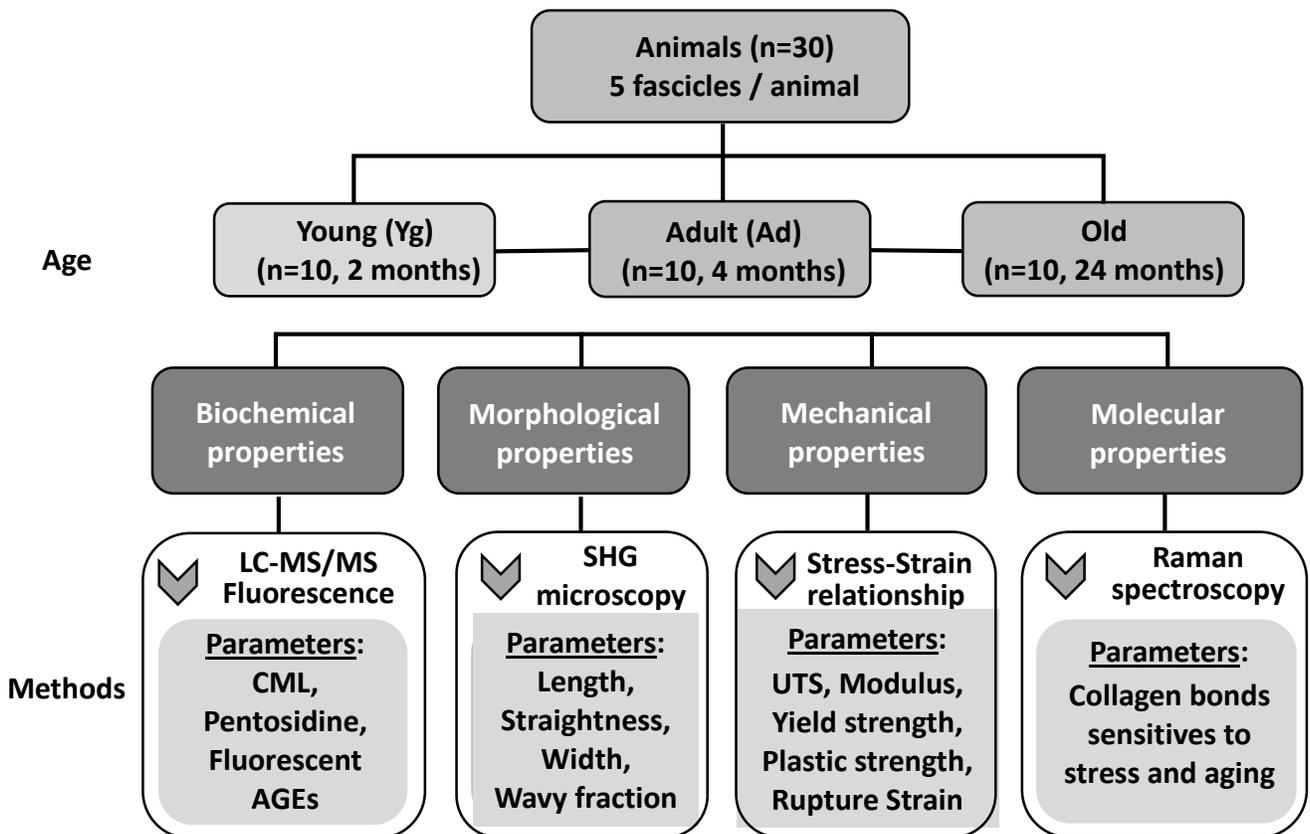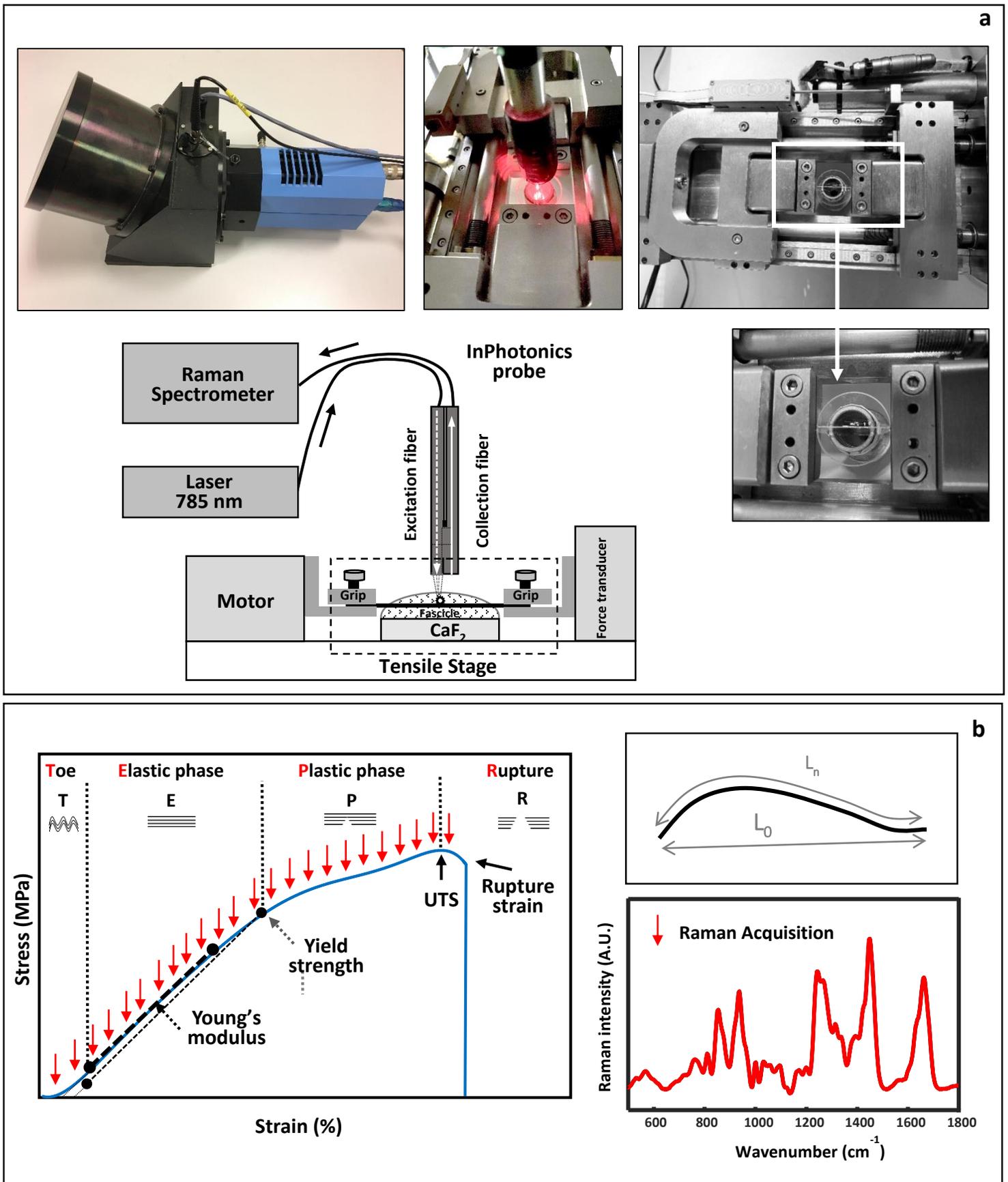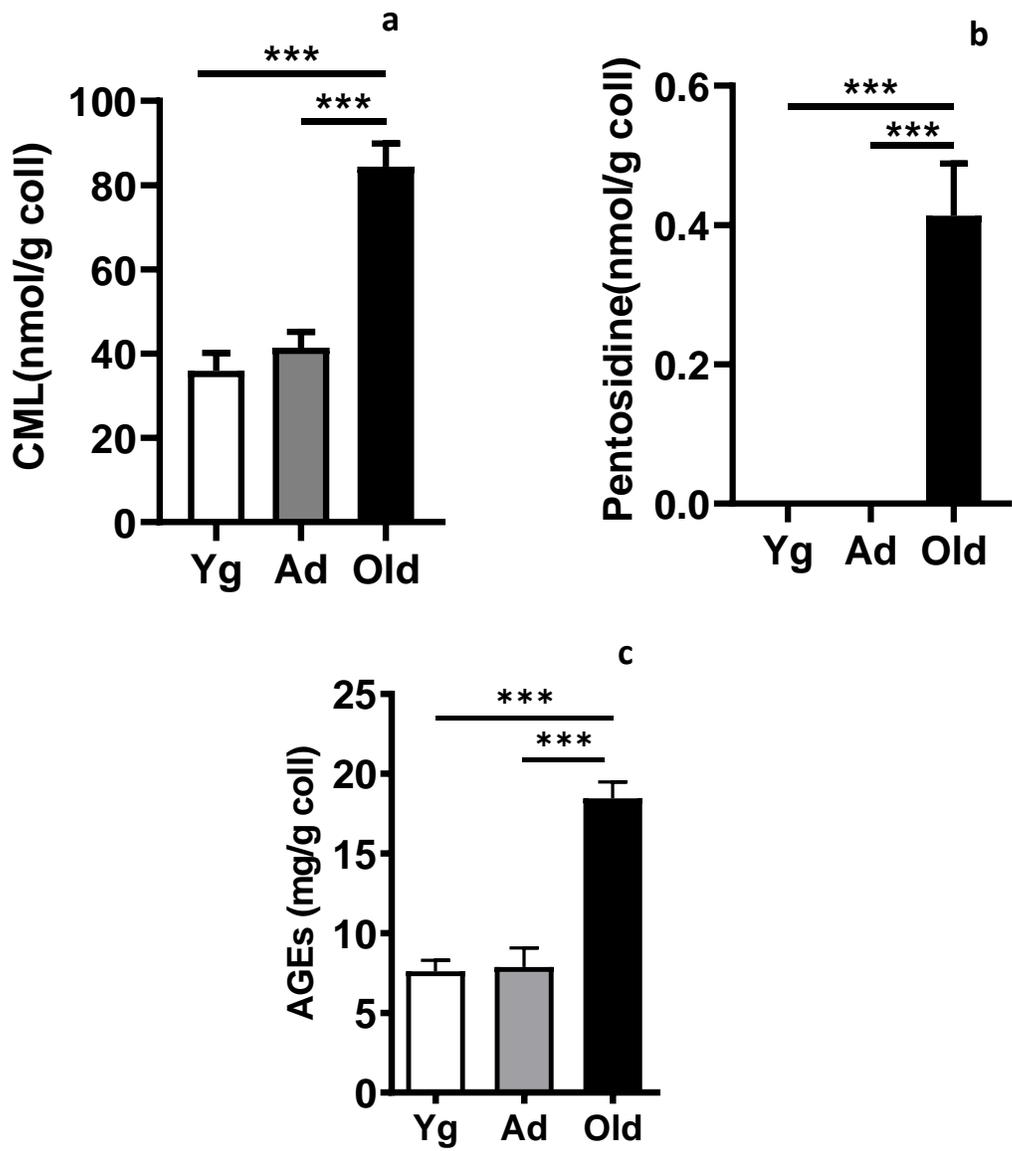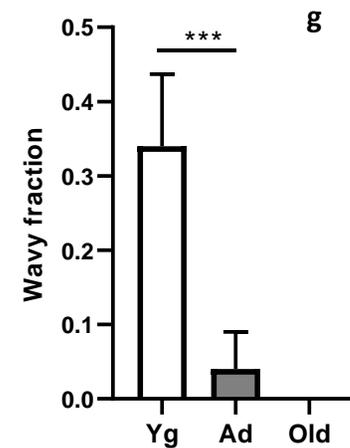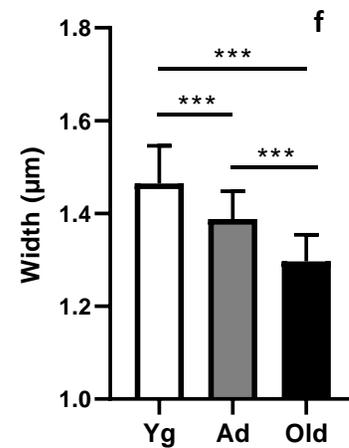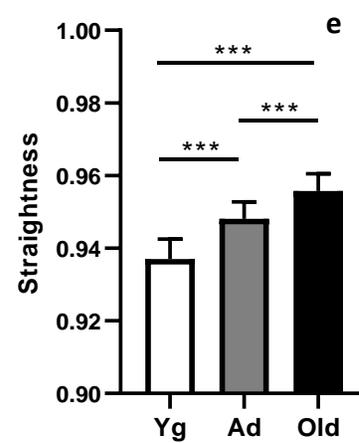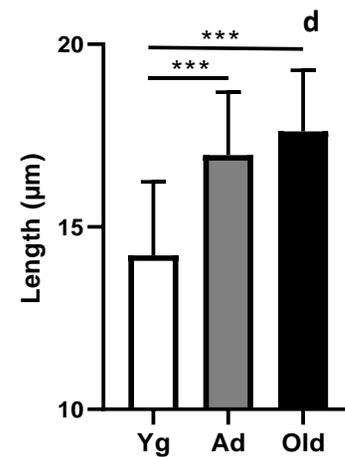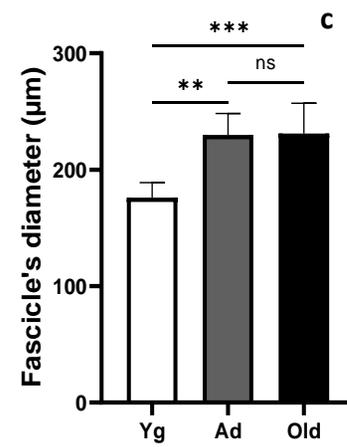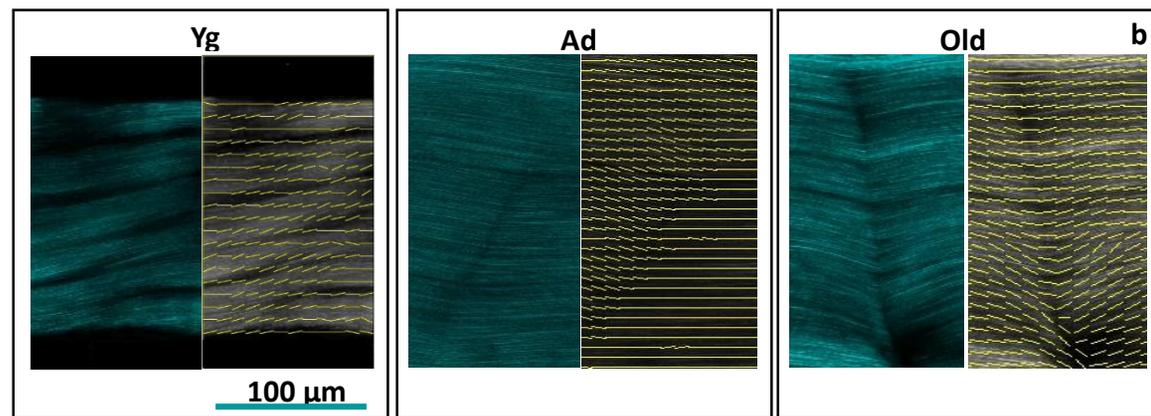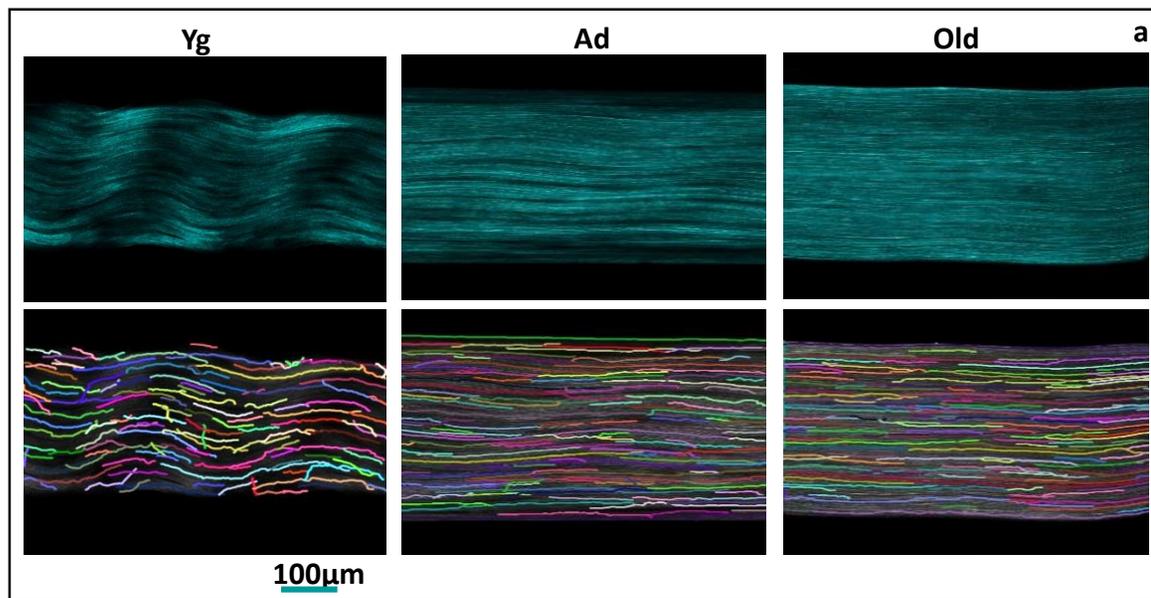
Figure 2

Figure 3

Figure 4
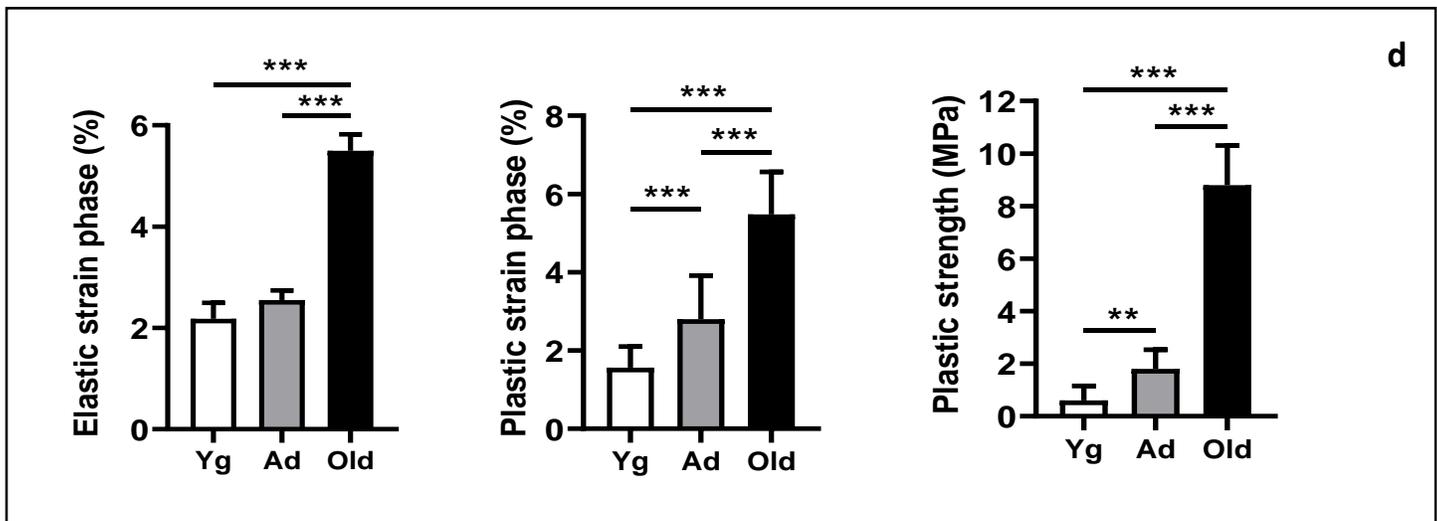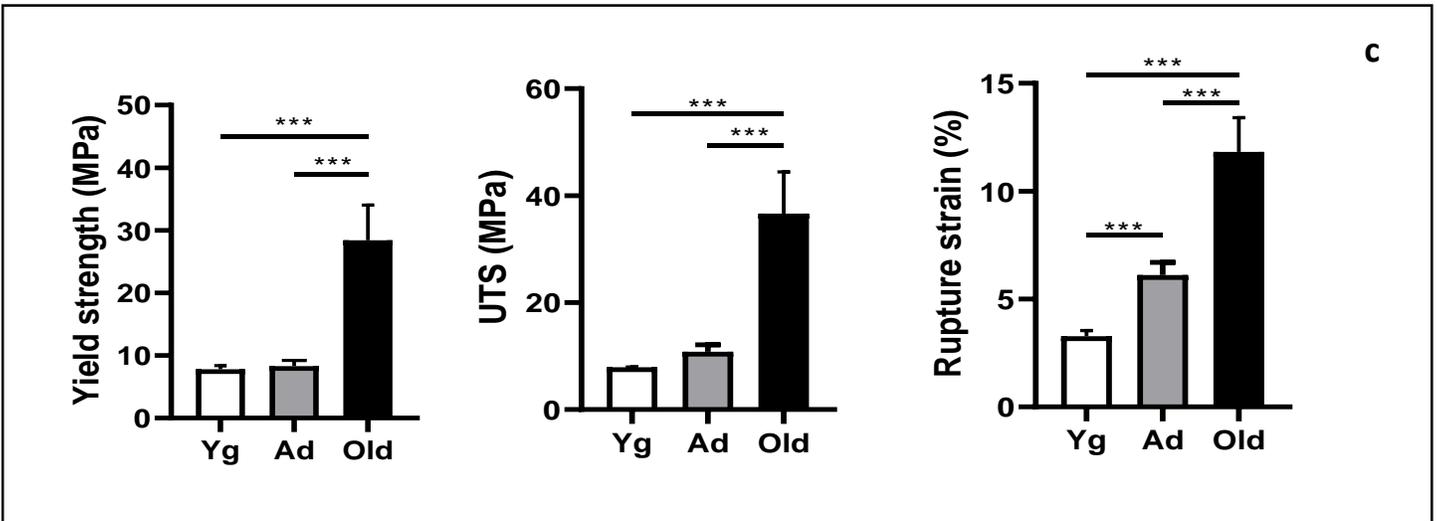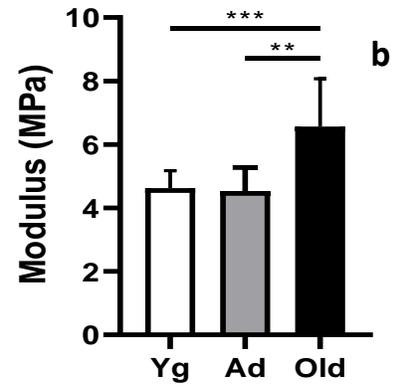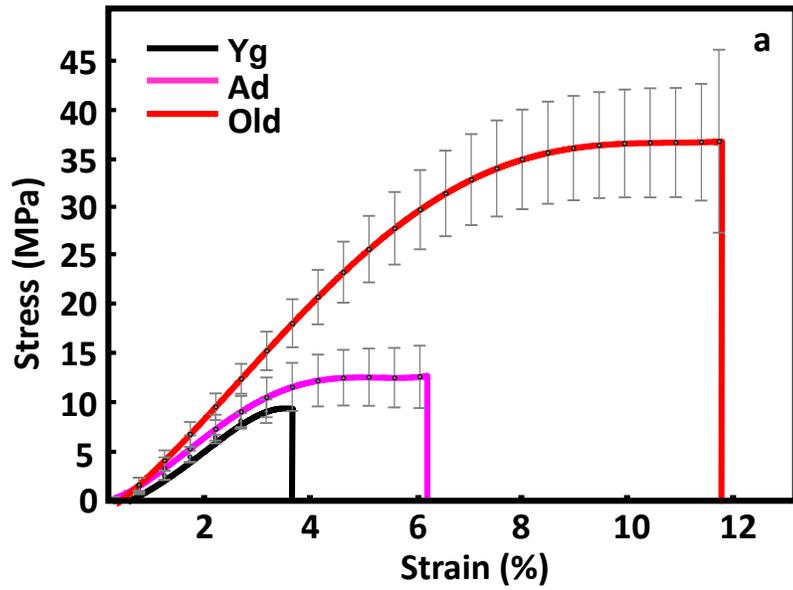
**Figure 5**
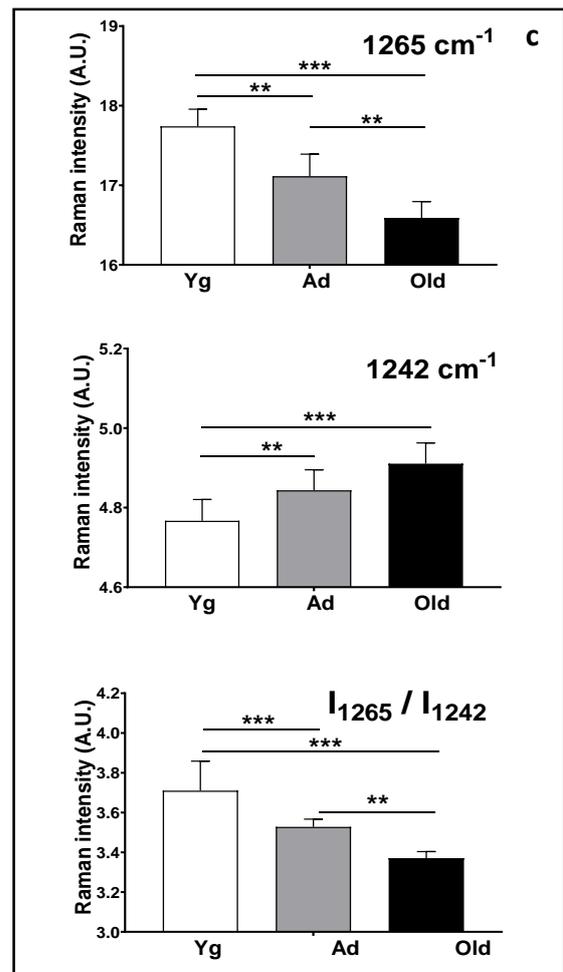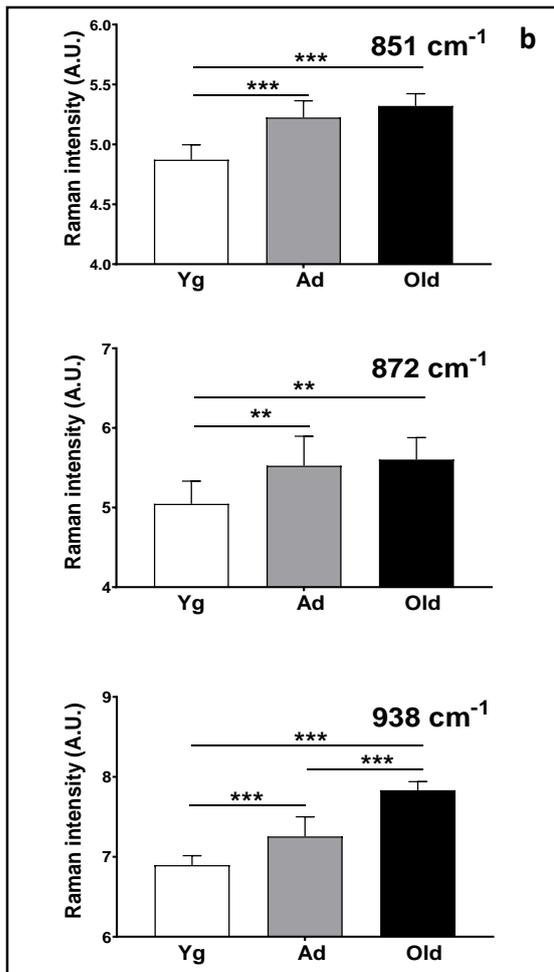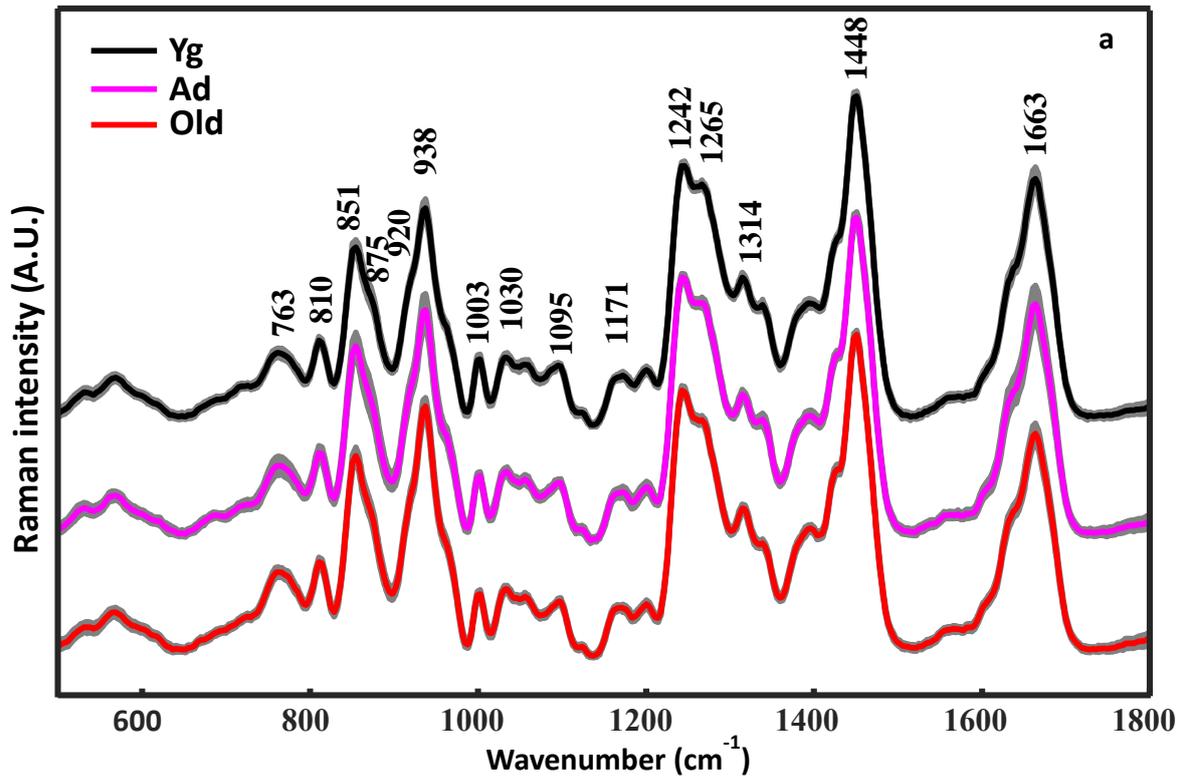
Figure 6
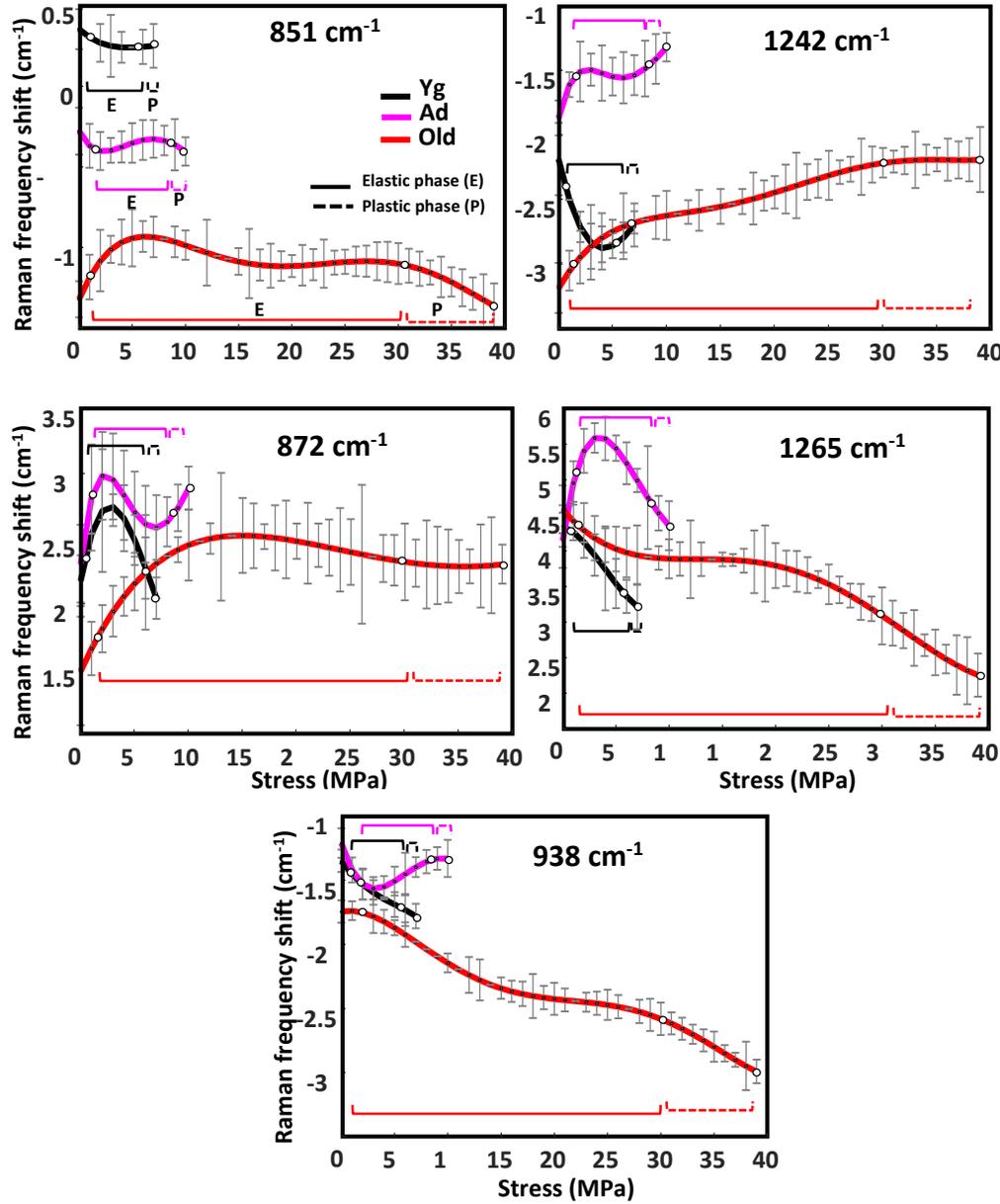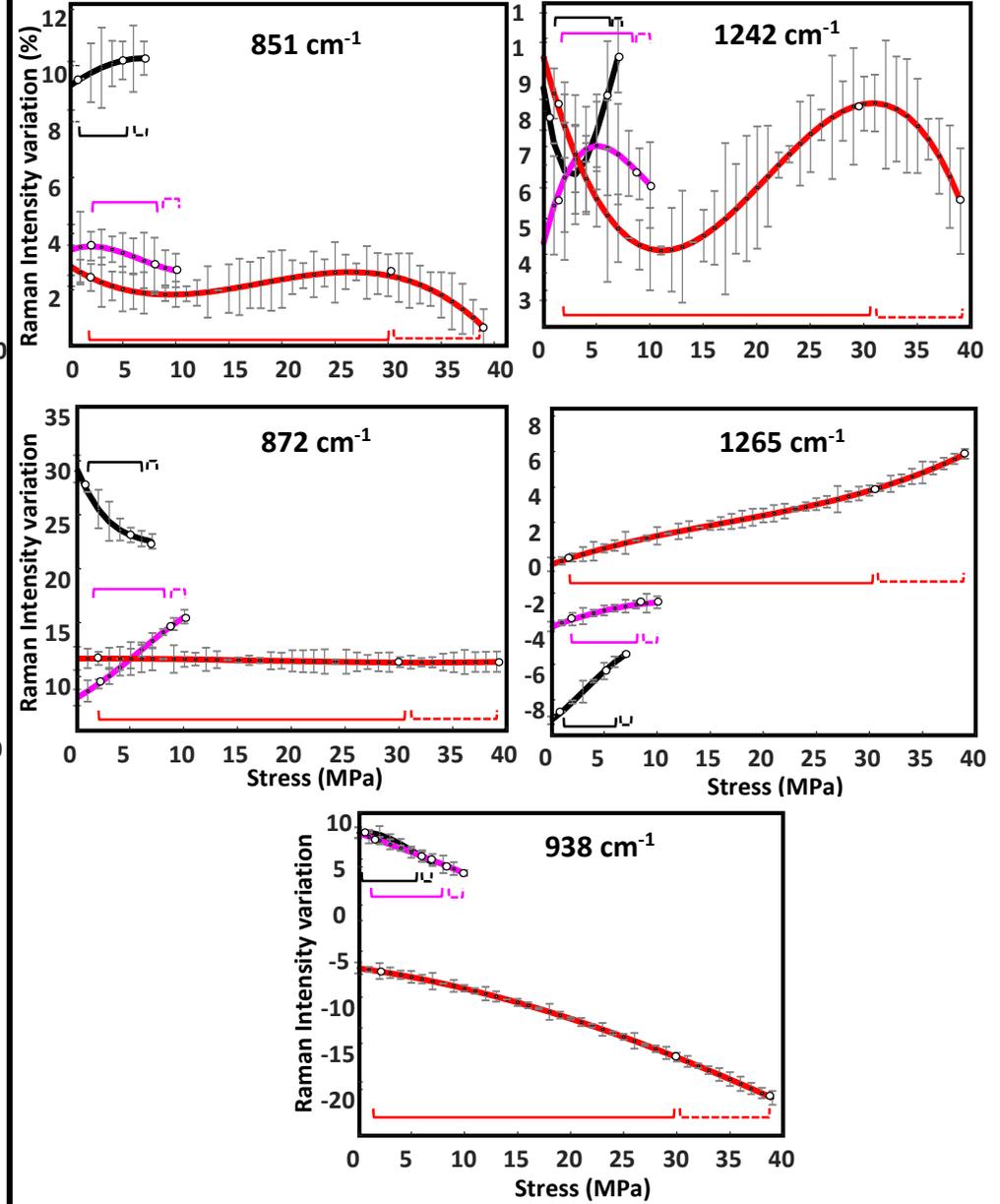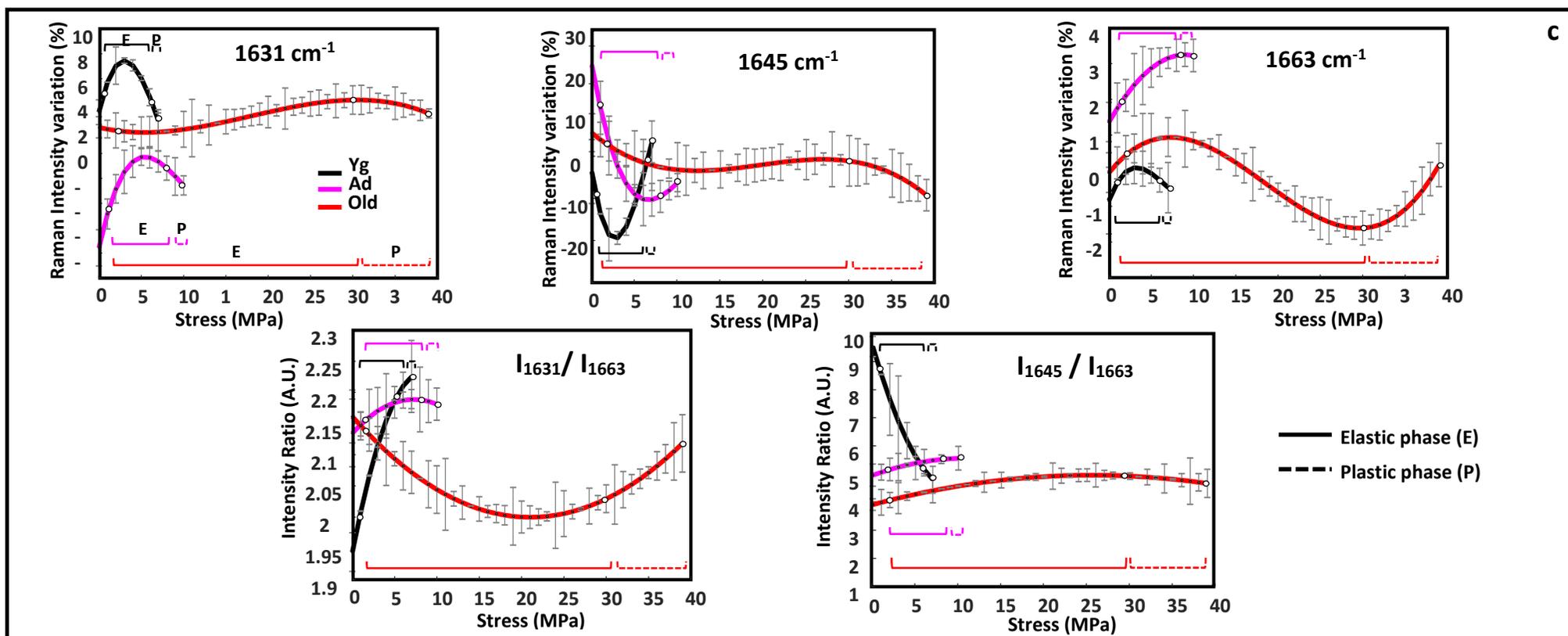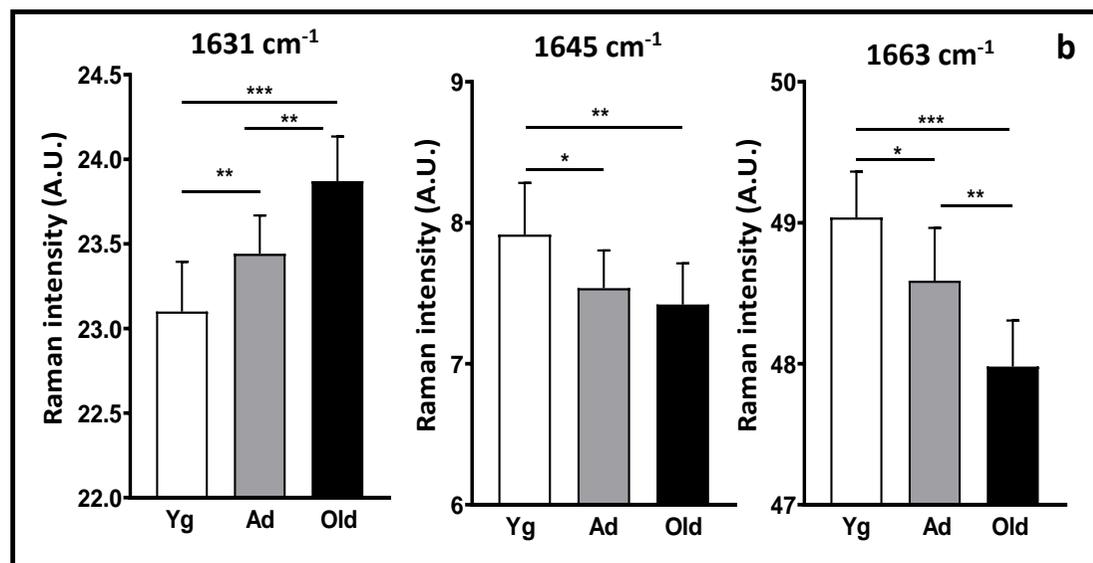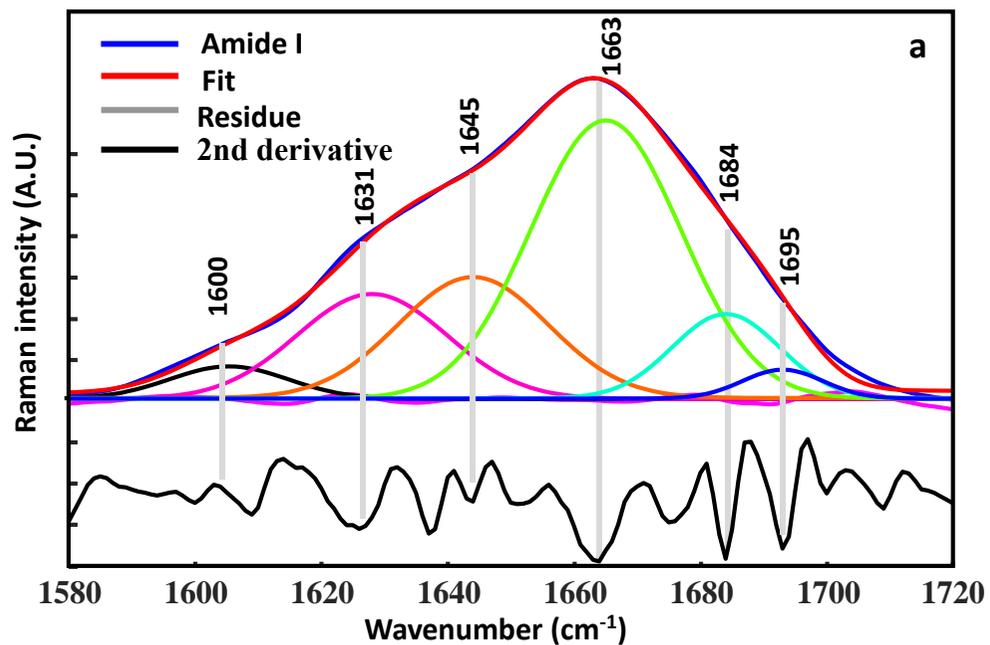
Figure 7

Figure 8

Table 1 : Stress and Strain contributions of Toe, elastic and plastic phases for Yg, Ad, and Old RTTFS

Stress (Mpa)	Phase /Age	Yg	Ad	Old
	Toe	0 - 0.9	0 – 1.1	0 – 1.6
	Elastic	0.9 - 7.6	1.1 – 8.2	1.6 – 28.0
	Plastic	7.8 - 8.0	8.3 – 10.8	28.4 – 36.7

Strain (%)	Phase /Age	Yg	Ad	Old
	Toe	0 - 0.4	0 - 0.3	0 - 0.5
	Elastic	0.4 - 2.6	0.3 - 2.8	0.5 – 6.0
	Plastic	2.7 – 3.2	3.0 – 6.0	6.3 - 11.8

Table 2. Raman bands assignment of type I collagen.

Band frequency (cm^{-1})	Assignment
1663	Amide I ν(C=O)
1448	δ(CH$_2$,CH$_3$),
1314	δ (CH)
1265	Amide III δ(NH$_2$)
1242	Amide III (C-N)
1171	ωCH2, tNH2, rNH3+
1095	δ NCH Pro
1030	ν CN Pro
1003	Phe
938	ν(C-C) of protein backbone
920	ν(C-C) of Pro ring
875	ν(C-C) of Hyp ring
851	ν(C-C) of Pro ring
810	ν(C-C) of protein backbone
763	δCOO-

ν stretching, δ deformation, ω wagging, t twist, r rocking.

Chronological aging

Rat tail tendon fascicles (RTTFs)

Age (months) 0 2 4   24   Natural death

Young   Adult   Old

SHG images

Morphological changes
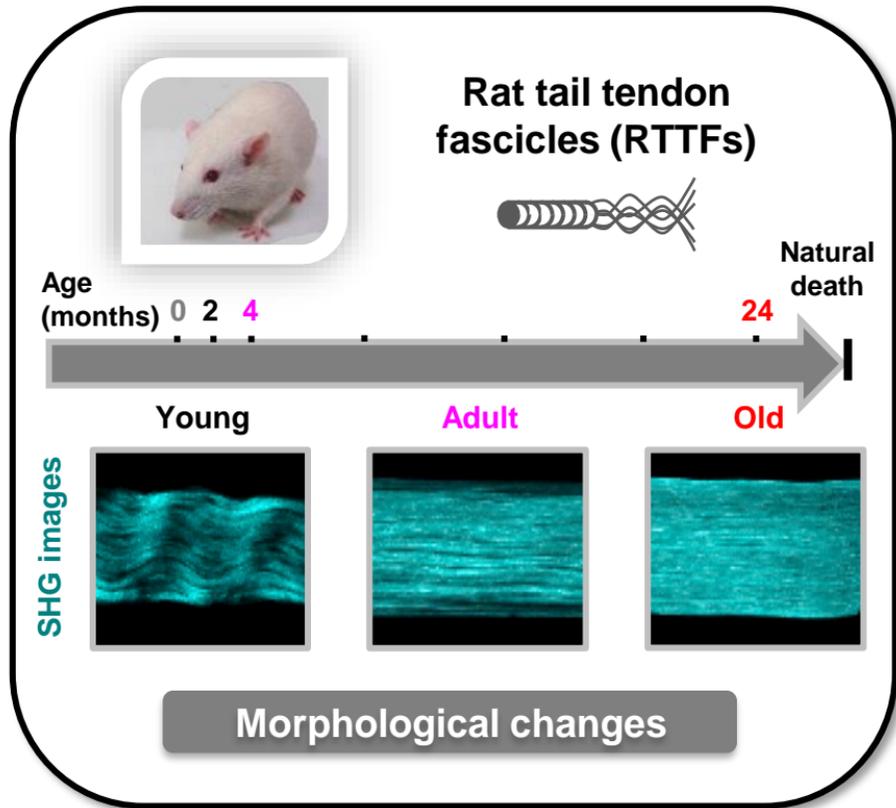
Integrated approach

Molecular properties

Raman spectrometer

785 nm Laser

Fiber probe

Motor

Tensile Stage

Mechanical properties
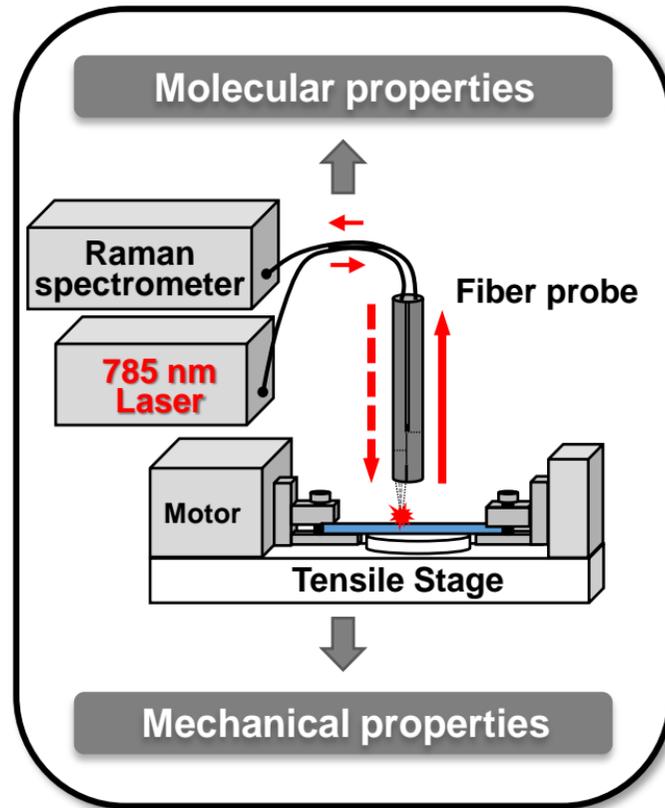
Molecular and mechanical relationship

Raman spectra

Young
Adult
Old

800 1000 1200 1400 1600

Stress-strain curve

Stress (MPa)

Strain (%)

collagen bands

Intensity

Stress (MPa)

Frequency shift

Stress (MPa)